RESEARCH

The potential involvement of inhaled iron (Fe) in the neurotoxic effects of ultrafine particulate matter air pollution exposure on brain development in mice

Marissa Sobolewski[1], Katherine Conrad[1], Elena Marvin[1], Matthew Eckard[2], Calla M. Goeke[1], Alyssa K. Merrill[1], Kevin Welle[3], Brian P. Jackson[4], Robert Gelein[1], David Chalupa[1], Günter Oberdörster[1] and Deborah A. Cory-Slechta[1*]

Abstract

Background: Air pollution has been associated with neurodevelopmental disorders in epidemiological studies. In our studies in mice, developmental exposures to ambient ultrafine particulate (UFP) matter either postnatally or gestationally results in neurotoxic consequences that include brain metal dyshomeostasis, including significant increases in brain Fe. Since Fe is redox active and neurotoxic to brain in excess, this study examined the extent to which postnatal Fe inhalation exposure, might contribute to the observed neurotoxicity of UFPs. Mice were exposed to 1 $\mu g/m^3$ Fe oxide nanoparticles alone, or in conjunction with sulfur dioxide (Fe (1 $\mu g/m^3$) + SO_2 (SO_2 at 1.31 mg/m^3, 500 ppb) from postnatal days 4–7 and 10–13 for 4 h/day.

Results: Overarching results included the observations that Fe + SO_2 produced greater neurotoxicity than did Fe alone, that females appeared to show greater vulnerability to these exposures than did males, and that profiles of effects differed by sex. Consistent with metal dyshomeostasis, both Fe only and Fe + SO_2 exposures altered correlations of Fe and of sulfur (S) with other metals in a sex and tissue-specific manner. Specifically, altered metal levels in lung, but particularly in frontal cortex were found, with reductions produced by Fe in females, but increases produced by Fe + SO_2 in males. At PND14, marked changes in brain frontal cortex and striatal neurotransmitter systems were observed, particularly in response to combined Fe + SO2 as compared to Fe only, in glutamatergic and dopaminergic functions that were of opposite directions by sex. Changes in markers of trans-sulfuration in frontal cortex likewise differed in females as compared to males. Residual neurotransmitter changes were limited at PND60. Increases in serum glutathione and Il-1a were female-specific effects of combined Fe + SO2.

Conclusions: Collectively, these findings suggest a role for the Fe contamination in air pollution in the observed neurotoxicity of ambient UFPs and that such involvement may be different by chemical mixture. Translation of such results to humans requires verification, and, if found, would suggest a need for regulation of Fe in air for public health protection.

*Correspondence: deborah_cory-slechta@urmc.rochester.edu

[1] Department of Environmental Medicine, University of Rochester Medical Center, Rochester, NY 14642, USA
Full list of author information is available at the end of the article

Background

Numerous epidemiological studies now associate exposures to air pollution (AP) with various neurodevelopmental disorders, including autism spectrum disorder (ASD), schizophrenia (SCZ) and attention deficit hyperactivity disorder (ADHD), all male-biased disorders. Experimental animal models increasingly provide biological plausibility for these associations [1–9]. In our studies in mice that underwent early postnatal exposures (equivalent to human third trimester brain development [10, 11]) to concentrated ambient ultrafine particles (UFPs), numerous and persistent male-specific or male-biased neuropathological changes and alterations in behavioral functions were observed, including ventriculomegaly, elevated brain glutamate levels, reductions in size and myelination of corpus callosum (the largest white matter tract in brain), increases in cytokine levels, and behavioral deficits including impulsive-like behavior [12–16]. When such exposures were carried out gestationally [17–19], ventriculomegaly was still observed, although in this period of exposure it was seen in both sexes, as was, in direct contrast to postnatal exposures, an increase in the size and myelination of corpus callosum, with collective effects that were more female-biased. These pathological features are consistent with numerous neurodevelopmental disorders [20–29] and thereby underscore the need to understand the components of air pollution that result in this neurotoxicity and how the impacts of these different components may differ by sex.

Analyses of filters from exposure chambers in our studies revealed the presence of multiple metals and trace elements in the AP exposures that could lead to brain metal dyshomeostasis [30]. Iron (Fe) is the metal of greatest abundance in the atmosphere [31] and thus is often a dominant component of the trace element levels of particulate matter, with concentrations clearly differing by geographical and industrial source. Indeed, a study from Korea reported that Fe dominated the $PM_{2.5}$ mass in subway stations at a concentration of > 100 μg/m^3 [32] while New York city subways were found to range from 141 to 329 μg/m^3 [32]. A study from China reported median Fe concentrations in outdoor air samples in Bejing at concentrations of 0.614 μg/m^3 in August and 0.378 μg/m^3 in December [33]. In a comparative study, Fe concentrations in Lodz Poland averaged 0.677 μg/m^3, and corresponding values for Milan averaged 0.353 μg/m^3 [34] whereas values from Karachi Pakistan averaged 3.175 μg/m^3 [35]. Data from the U.S. Environmental Protection Agency

Speciate Database cited Fe emissions of 103,000 tons/year and 1210 μg/m^3/day [36].

Correspondingly, ICP-MS analyses of brain sections from male mice exposed postnatally to concentrated ambient ultrafine particles revealed brain metal dyshomeostasis, characterized by marked elevations of metals and trace elements in brain, including Fe and sulfur (S), but that also included increases in calcium (Ca), copper (Cu) and aluminum (Al) [30]. Increases in brain Fe were also found in response to gestational exposures, particularly in female offspring [19]. While both Fe and S are requisite to brain development [37–42], they are also detrimental in excess [43–49]; Fe in air pollution has been shown to be redox active and capable of inducing oxidative stress [50]. Mechanisms to control Fe uptake in brain are not operative during early periods of brain development [51], leaving fetal brain susceptible to such exposures.

Metal dyshomeostasis has been implicated in neurodevelopmental disorders including autism, schizophrenia and attention deficit disorder [52–57]. While in the case of neurodevelopmental disorders such reports have largely been based on serum or hair analyses, studies have reported excess Ca levels in post-mortem neocortical tissue from individuals that had been diagnosed with ASD [58], and serum metal changes have been related to markers of inflammation in autism as well [59]. Understanding of changes in brain metals specifically and their relationships to neurodevelopmental disorders is not clear, particularly as directions of changes in metals in serum do not necessarily correspond to alterations in levels of those metals in brain [60–64].

Based on these findings, the current study sought to determine the extent to which the Fe component, via Fe oxide nanoparticle inhalation, serves as a basis for the neurotoxicity produced by postnatal inhaled ambient ultrafine particle exposures. In ambient air, Fe concentrations are correlated with sulfate content, based on sulfate's ability to mobilize Fe from its oxide form [65]. Further, an early study [66] reported that sulfur dioxide (SO_2) increased the uptake of Fe into the central nervous system (CNS) and altered its distribution among different cell types. Consequently, in other cohorts of mice, Fe oxide nanoparticle exposures were carried out concurrently with SO_2 exposure $(Fe + SO_2)$ and assessments of metal dyshomeostasis, trans-sulfuration pathways, serum cytokines and brain neurotransmitter levels were compared to effects previously observed in response to

Sobolewski *et al. Particle and Fibre Toxicology*   (2022) 19:56

Page 3 of 19

ambient UFP exposures from our prior studies [12, 14, 15, 67].

Methods and materials

Animals

C57BL6/J mice were kept, bred and exposed as previously described [12, 14, 68–76]. Briefly, mice were bred monogamously with sires removed following sperm plug identification. Pups were housed solely with the dam and were weaned on postnatal day (PND) 21. Mice were housed in standard mouse caging with 1/8″ high performance bedding (BioFresh, WA, USA), under a 12 h light-dark cycle, maintained at 22 ± 2 °C, and fed standard rodent chow at the University of Rochester Medical Center. Following weaning, offspring were pair housed by sex and treatment group for the duration of the study. All mice were used and treated via protocols approved by the University of Rochester Medical Center Institutional Animal Care and Use Committee and Committee on Animal Resources (approval # 102,208 / 2010-046E), and in accordance with NIH guidelines. Mice were euthanized at either PND 14, 30, 60 or 90 and tissue harvested for various analyses.

Fe and Fe + SO$_2$ exposures

Mice were exposed either to iron (Fe) and and or Fe and sulfur (S); specifically, to Fe oxide (Fe) nanoparticles alone or with sulfur dioxide (SO_2) gas from postnatal days 4–7 and 10–13 for 4 h. The exposures were to Fe vs Fe + SO$_2$ were carried out at separate times, each with its corresponding filtered air control group. Mice were exposed in exposure cages via whole body inhalation. For this study, the intended SO_2 concentration was 1.31 mg/m^3, and the intended Fe concentration was 1.0 µg/m^3. The Fe concentration was chosen to be within the range of values cited for outdoor Fe levels as cited above [33–35]. The SO_2 concentration was based on the U. S. Environmental Protection Agency secondary standard for SO_2. Fe-oxide UFP particles were generated by electric spark discharge between two 99.99999% pure iron rods (3N5 Purity, ESPI Metals, Ashland, OR, USA) using a GFG-1000 Palas generator (Palas GmbH, Karlshrue, Germany), and fed into a compartmentalized whole-body mouse exposure chamber, while HEPA-filtered air was delivered to the control chamber, as in prior studies in our inhalation facility [77]. Passing the airborne particles through a deionizer (Isotope Po-210, model P-2031, NRD, Grand Island, NY, USA) was used to bring particle charge to Boltzmann equilibrium. Particle number concentration was adjusted by altering electric spark discharge frequency. Aerosol number concentration and particle size were monitored in real-time using a Condensation Particle Counter (CPC, model 3022, TSI Inc, St Paul, MN, USA)

and Scanning Mobility Analyzer (SMPS, model 3934 TSI Inc, St Paul, MN, USA) respectively. The Fe-oxide particles were generated by adding a low flow of oxygen (~ 50 mL/min) into the argon flow (~ 5 L/min) entering the spark discharge chamber. The oxygen concentration of 21% in the exposure chamber was verified by an O_2 sensor (MAXO2 -250E, Maxtec, Salt Lake City, UT, USA). This procedure produced particle sizes exclusively in the ultrafine size range with a count median diameter (CMD) of approximately 12–14 nm. Mass concentrations were determined by ICP-OES analysis of Fe on nitrocellulose membrane filters (0.8 micron, AAWP02500, Millipore Ltd., Tullagreen, Cork, IRL) collected daily (5 L/min for 60 min., 300L total volume) from the filtered air and ultrafine Fe-oxide particle exposure chambers. For the concurrent SO_2 exposures, SO_2, compressed in gas cylinders (EPA Protocol Standard, 50 ppm, Airgas East, Radnor, PA, USA), was diluted with filtered air and then bled into (200 ml/min) the Fe-oxide containing conduit to achieve final desired concentrations for Fe + SO$_2$ exposures. This Fe-oxide/SO$_2$ mixture was fed into the whole-body exposure chamber at 25–30 L per minute. SO_2 concentrations were continuously monitored and recorded with an SO_2 gas monitor (model 43C, Thermo Environmental Instruments Inc., Franklin, MA, USA). Intended Fe and Fe + SO$_2$ concentrations were chosen to be consistent with the lower reported concentrations as cited above.

Metal analyses

Pre-weighed tissue samples were acid digested in 1.5 ml Eppendorf tubes using a Fisher hot-block. A sample-dependent range of 200–500 µl of 9:1 HNO3:HCl (Optima grade, Fisher Scientific) was added to the tubes, which were then heated at 80 C for 1 h. Olfactory bulbs (1–9 mg) were digested with 200 µl acid mix and diluted to a final volume of 2 ml with deionized water and the final dilution weight recorded. Cortex (48–103 mg) and lung (15–96 mg) were digested with 500 µl acid mix and diluted to a final volume of 5 ml with deionized water and the final dilution weight recorded. Six blanks and 6 reference material samples (NIST 2976 Mussel Tissue, 6–18 mg) were included in the digest and diluted to 5 ml.

  Digested samples were analyzed by ICP-MS (Agilent 8900, Wilmington, DE) in helium and oxygen modes. Nist-traceable primary standards were used to construct a multi-element calibration curve, second source standards were used for a calibration check repeated after each calibration and every 10 samples. USGS water proficiency samples (P76, T-245) were used as a further calibration check and repeated three further times during the analysis. Five analytical duplicates and five analytical spikes were also performed and data reported in ug/g or

Sobolewski *et al. Particle and Fibre Toxicology*   (2022) 19:56

Page 4 of 19

ng/g depending upon the metal. Quality control data is summarized in Additional file 1: Table 1.

Bronchoalveolar lavage (BAL) procedure and analysis

Lungs were excised with the trachea, then lavaged 10 times with warmed sterile 0.9% saline (10×1 mL). For this purpose, the first two lavage washes were reserved separately from the rest to prevent cell dilution. BAL fluid was centrifuged at $400 \times g$ for 10 min to separate out the cell fraction. Supernatants from lavages 1–2 were used for measurements of total protein (microBCA, Thermo-Fisher Scientific) and lactate dehydrogenase (LDH) activity (Sigma Aldrich).

Serum glutathione and IL-1a

Serum glutathione was measured using the Glutathione Colorimetric Detection Kit (Arbor Assays, Cat. K006-H1). The kit was run, as described, and each sample was run twice to measure both oxidized and total glutathione. Samples were run in duplicate and counterbalanced across the plate based on sex and treatment group.

Serum cytokines (IL-1a, IL-1b, IL-2, IL-6, IL10, IFN-g and TNF-a) were measured using Mouse Cytokine Grpl 7-plex luminex Kit (Bio-Rad, Cat. Y60000017G) as described in Bio-Plex Pro Assays for use with Mouse and Rat Cytokine Assays, instruction manual #10,014,905. Limits of detection for the $Fe+SO_2$ samples were 0.508, 1.99, 1.397. 0.411, 13.197, 3.331 and 230.587 pg/ml, and for the Fe samples, were 2.248, 1.425, 1.335, 1.967, 4.694, 0.885 and 54.706, respectively. For both cohorts, samples were run in duplicate and counter-balanced across the plate based on sex and treatment group. Sample and standard duplicates calculated coefficients of variation were below 15%.

Brain neurotransmitter and trans-sulfuration analyses

Striatal concentrations of various neurotransmitters were quantified by the University of Rochester Mass Spectrometry Core: DA, DOPAC, HVA, Tyrosine (Tyr), Glutamate (Glu), GABA, Glutamine (Gln), Kynurenic Acid (Kyn), 5-HT, 5-HIAA, and Tryptophan (Trp). Tissues were thawed, weighed, diluted in 75 µL of ice-cold acetonitrile (50%, v/v) and homogenized for 10 s via ultrasonication (SLPe digital sonifier, Branson Ultrasonics Corp., Danbury, CT.). The homogenate was centrifuged at 10,000 g (4 °C) for 20 min. The resulting supernatant was collected and centrifuged at 10,000 g (4 °C) for 20 min, after which the new supernatant was collected and stored at -80 °C until analysis.

Stock solutions of DA, DOPAC, HVA, Glu, GABA, Glu, Kyn, 5-HT, 5-HTP, 5-HIAA, and Trp (Sigma Aldrich) were made at 5 mg/mL in ddH$_2$O, with the exception of Tyr, which was made in 0.2 M HCl. A standard mixture was created in ddH$_2$O, with analyte concentrations varying in accordance with prior range-finding studies, in order to account for region-specific variations in endogenous neurotransmitters. This stock solution was derivatized using 13C6 benzoyl chloride (BzCl, Sigma Aldrich) using a method adapted from Wong et al. [78], to create internal standards for each individual neurotransmitter. The derivatized internal standard mixture was aliquoted and frozen at -80 °C for long term storage. Internal standard aliquots were thawed, then diluted in 50% acetonitrile with 1% sulfuric acid prior to being added to the samples. Prior to analysis, samples were derivatized following the same procedure. In brief, samples were centrifuged at 16,000 g for 5 min to remove debris, then 20 µL of resulting supernatant was placed in a clean LoBind tube (Eppendorf). Next, 10 µL of 100 mM sodium carbonate, 10 µL of 2% BzCl in acetonitrile, and 10 µL of the respective internal standard was added in sequence. 50 µL of ddH$_2$O was then added to reduce the organic concentration prior to injection. Samples were centrifuged once more to pellet any remaining protein, and the supernatant was added to a clean autosampler vial.

LC-MS/MS analysis was carried out by a Dionex Ultimate 3000 UHPLC coupled to a Q Exactive Plus mass spectrometer (Thermo Fisher). Analytes were separated on a Waters Acquity HSS T3 column. The mobile phases were: A) 10 mM ammonium formate in 0.1% formic acid, and B) acetonitrile. The flow rate was set to 400 µL/min and the column oven was set at 27 °C. After 5 µL of each sample was injected, the analytes were separated using a 12 min multi-step gradient. The Q Exactive Plus was operated in positive mode, and a parallel reaction monitoring method (PRM) was used to detect derivatized molecules. Fragment ions were extracted with a 10 ppm mass error using the LC Quan node of the XCalibur software (Thermo Fisher). Endogenous analyte peak areas were compared to those of each internal standard to determine relative abundance. These values were then divided by wet weight of the sample and then calculated by air control to yield percent of control values.

Statistical analysis

Levels of serum cytokines, striatal and frontal cortical neurotransmitters (area ratio/weight values), serum oxidized glutathione and metal levels in tissues were analyzed using t tests comparing the Fe or $Fe+SO_2$ exposed mice to their corresponding control group. These analyses were carried out separately by sex, as our prior studies consistent reveal sex differences in response to air pollution [12, 14, 68]. To assess metal dyshomeostasis, multivariate correlation analysis was carried out across metals for lung, olfactory bulb and cortex. Body weights

Sobolewski *et al. Particle and Fibre Toxicology*   (2022) 19:56

Page 5 of 19

over the course of exposure to $Fe + SO_2$ were analyzed using repeated measures analyses of variance based on Pearson's correlation coefficients with time as a within-group factor and treatment as a between-group factor.

All data were analyzed using JMP Pro16; outliers were evaluated using a Grubb's test (Prism Graph Pad); no more than one outlier was removed from any group (treatment/sex), and the mean value of the remaining values was substituted. A *p*-value of ≤ 0.05 was considered significant; marginal effects where reported reflect a *p* value of ≤ 0.10.
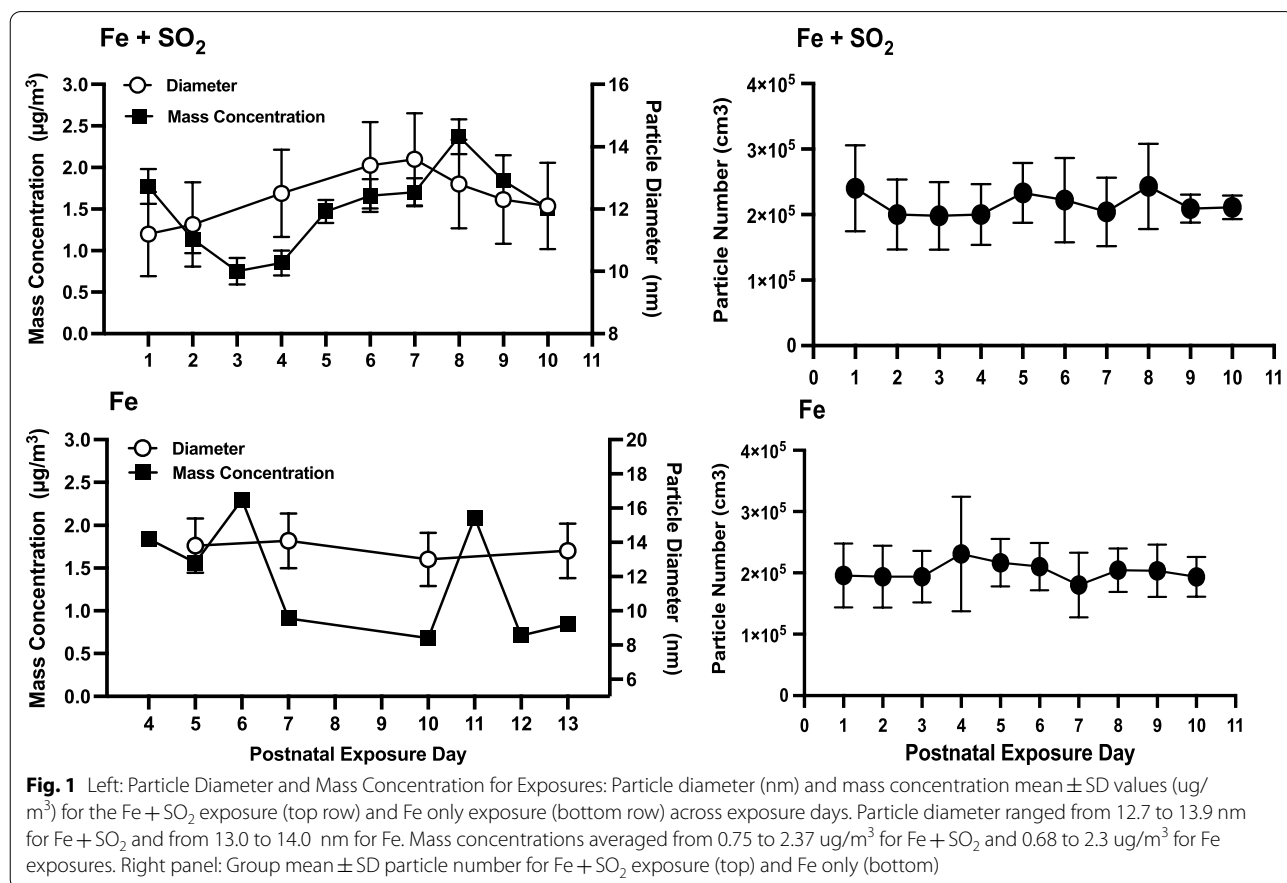
Results

Exposure characteristics

Particle diameter and mass as well as particle number for each of the two exposures are shown in Fig. 1. For $Fe + SO_2$ (Fig. 1 top, $Fe + SO_2$), Fe mass concentrations across days ranged from 0.75 to 2.37 $\mu g/m^3$ over the exposure period, producing an average concentration of 1.51 $\mu g/m^3$, given the known oxidation of Fe with relative contribution of oxygen to these particles and the intended target of 1.0 $\mu g/m^3$ inhaled Fe. Count Median Diameter (CMD) particle size varied from 11.2 to 13.6 nm, with an average Geometrical Standard Deviation (GSD) of 1.4,

which is within the ultrafine size range. The daily particle number concentration average $\pm$ standard deviation was 2.16E+05 $\pm$ 0.17E+05 part/cm^3, a consistently high number concentration exposure of pure Fe particles, exceeding what would be seen in Fe ambient environmental exposure levels by number. Therefore, a large number to surface area ratio ($\mu m^2/cm^3$) consistently existed for these laboratory exposures, about 150 times that of a unit density sphere at a mass concentration of 1 ug/m^3. For Fe only exposure (Fig. 1 bottom), Fe particle mass concentrations were 10-day average = 1.42 $\mu g/m^3$, again given the known oxidation of Fe with relative contribution of oxygen to these particles with the intended 1 $\mu g/m^3$ target on average for inhaled Fe, with variation across the 10 days (range = 0.68–2.44 $\mu g/m^3$). The particle number concentrations were similar for Fe only exposures (10-day avg. $\pm$ st dev.: 2.03E+05 $\pm$ 0.14E+05 part/cm^3). Particle diameter was consistently between 13–14 nm (mean = 13.6 nm, GSD 1.6) indicating a consistent ultrafine aerosol, as intended.

Body weights

Body weights of the $Fe + SO_2$ group were over the course of the exposures as well as out to postnatal day 90 are

Fig. 1 Left: Particle Diameter and Mass Concentration for Exposures: Particle diameter (nm) and mass concentration mean $\pm$ SD values (ug/m^3) for the $Fe + SO_2$ exposure (top row) and Fe only exposure (bottom row) across exposure days. Particle diameter ranged from 12.7 to 13.9 nm for $Fe + SO_2$ and from 13.0 to 14.0 nm for Fe. Mass concentrations averaged from 0.75 to 2.37 ug/m^3 for $Fe + SO_2$ and 0.68 to 2.3 ug/m^3 for Fe exposures. Right panel: Group mean $\pm$ SD particle number for $Fe + SO_2$ exposure (top) and Fe only (bottom)

Sobolewski *et al. Particle and Fibre Toxicology*   (2022) 19:56

Page 6 of 19

shown in Fig. 2A. As can be seen, small but significant body weights reductions were seen in females exposed to $Fe + SO_2$ relative to female air control over the course of the exposure, while similar but non-significant trends were observed in males (female: $F(1,17) = 28.09$, $p < 0.0001$; males: $F(1,15) = 2.58$, $p = 0.13$). However, these differences had disappeared by postnatal day 90, at which time there were no significant differences in either sex. In the Fe only exposed group (Fig. 2B), body weights were obtained at postnatal day 14 and did not differ in relation to exposure in either sex (females: 6.18 ± 0.11 versus 6.33 ± 0.108 gm for air-exposed vs. Fe-exposed; males: 6.26 ± 0.15 versus 6.13 ± 0.14 gm for air-exposed versus Fe-exposed).

Lung markers

Bronchioalveolar lavage fluid was collected from $Fe + SO_2$ exposed pups to ascertain markers of lung function, including lactate dehydrogenase (LDH) and total protein levels, and corresponding values are shown in Fig. 2C. These assessments did not reveal any evident changes in response to $Fe + SO_2$ in either sex.
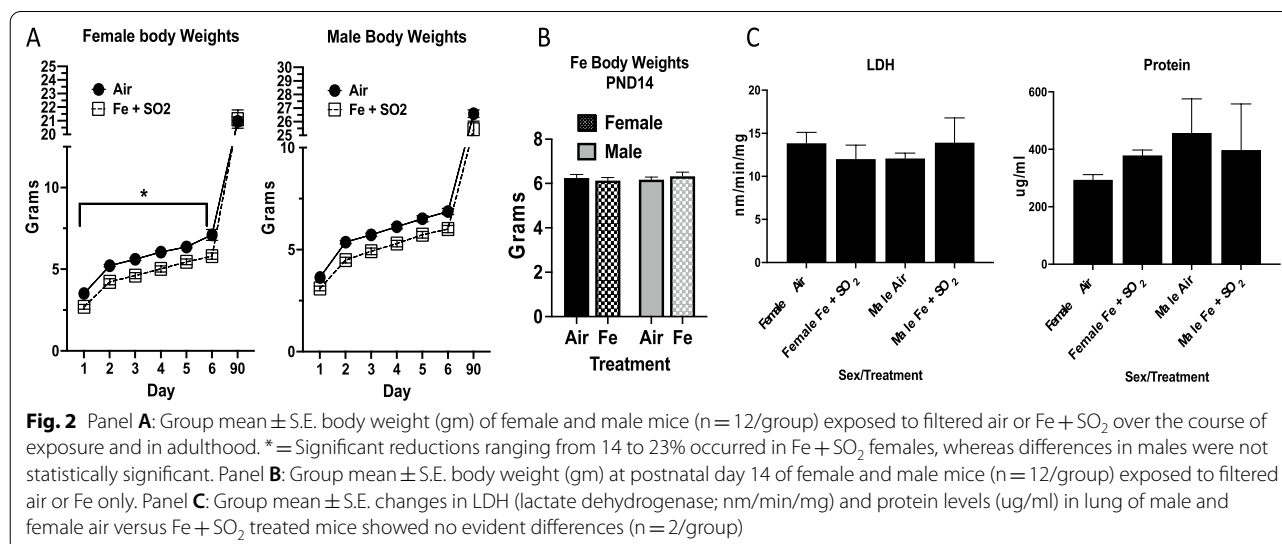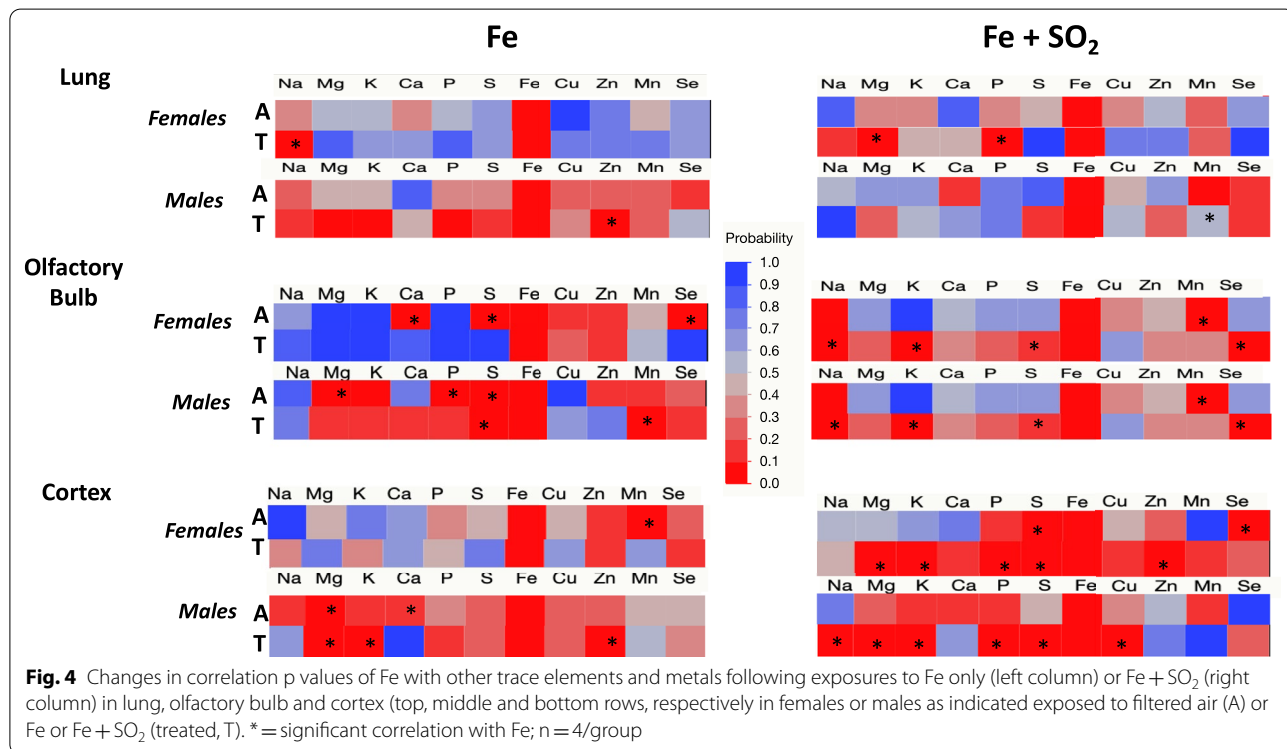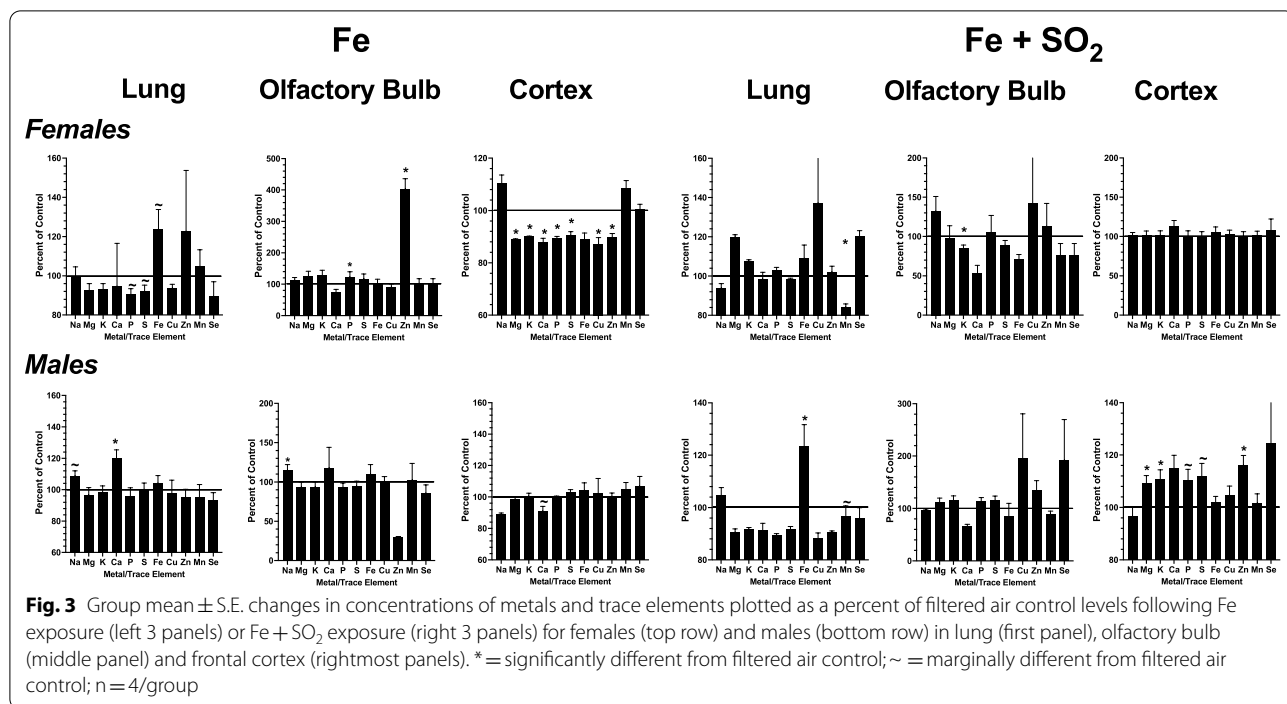
Metal levels and correlations of metals

Levels of metals and trace elements were quantified (µg/gm or ng/g of tissue) in lung, olfactory bulb and frontal cortex, and values are presented as percent of filtered air control levels in **Fig. 3**. After Fe only exposures, the most dramatic effects in females were found in frontal cortex, with reductions in levels of Mg, K, Ca, P, S, Cu and Zn (Mg: $F(1,6) = 27.4$, $p = 0.002$; K: $F(1,6) = 14.18$, $p = 009$; Ca: $F(1,6) = 5.998$, $p = 0.0499$; P: $F(1,6) = 12.13$, $p = 0.013$; S: $F(1,6) = 6.38$, $p = 0.045$; Cu: $F(1,6) = 20.6$, $p = 0.004$; Zn: $F(1.6) = 11.3$, $p = 0.015$), with a marked increase in Zn in

olfactory bulb $(F(1,6) = 82.86$, $p < 0.001)$, and marginal reductions of P and S in lung (P: $F(1,6) = 5.87$, $p = 0.051$; S $(F91,6) = 3.79$, $p = 0.099)$. In males, the only significant changes in response to Fe were marginal increases in Na $(F(1,6) = 5.81$, $p = 0.053)$ and Ca in lung $(F(1,6) = 11.49$, $p = 0.015)$ and a marginal reduction in Ca in frontal cortex $(F(1,6) = 4.13$, $p = 0.089)$.

Following $Fe + SO_2$ exposures, females showed significant reductions in Mn in lung and K in olfactory bulb (Mn: $F(1,6) = 6.28$, $p = 0.046$; K: $F(1,6) = 8.69$, $p = 0.026$). In males, a marked and significant increase in lung Fe was observed $(F(1,6) = 6.2$, $p = 0.047)$, while numerous changes were detected in frontal cortex, including significant increases in Mg, K and Zn (Mg: $F(1,6) = 6.54$, $p = 0.043$; K: $F(1,6) = 6.88$, $p = 0.039$; Zn: $F(1,6) = 17.13$, $p = 0.006)$ and marginal increases in P and S (P: $F(1,6) = 4.59$, $p = 0.076$; S: $F(1,6) = 5.08$, $p = 0.065)$. Thus, marked changes in metal concentrations in frontal cortex were seen in response to Fe only in females but after $Fe + SO_2$ exposure in males and the corresponding changes were opposite in direction.

To assess metal dyshomeostasis, correlations among metals within each region were examined. Figure 4 shows correlations of Fe with other metals in groups treated with Fe only (left column) or $Fe + SO_2$ (right column) for females and males exposed to either filtered air (A) or treatment (T: Fe or $Fe + SO_2$). In lung (Fig. 4 top row), Fe was not correlated with any other metal/element in air-exposed females. However, significant correlations emerged with Na post Fe only exposure, and with both Mg and P after $Fe + SO_2$ exposure. Similarly, Fe was not correlated with other metals/elements in lung of air-treated males; this was not altered by $Fe + SO_2$ treatment, while correlations with Zn emerged following Fe only.

Fig. 2 Panel **A**: Group mean ± S.E. body weight (gm) of female and male mice (n = 12/group) exposed to filtered air or $Fe + SO_2$ over the course of exposure and in adulthood. * = Significant reductions ranging from 14 to 23% occurred in $Fe + SO_2$ females, whereas differences in males were not statistically significant. Panel **B**: Group mean ± S.E. body weight (gm) at postnatal day 14 of female and male mice (n = 12/group) exposed to filtered air or Fe only. Panel **C**: Group mean ± S.E. changes in LDH (lactate dehydrogenase; nm/min/mg) and protein levels (ug/ml) in lung of male and female air versus $Fe + SO_2$ treated mice showed no evident differences (n = 2/group)

Sobolewski *et al. Particle and Fibre Toxicology*   (2022) 19:56

Page 7 of 19

Fig. 3 Group mean ± S.E. changes in concentrations of metals and trace elements plotted as a percent of filtered air control levels following Fe exposure (left 3 panels) or Fe + SO$_2$ exposure (right 3 panels) for females (top row) and males (bottom row) in lung (first panel), olfactory bulb (middle panel) and frontal cortex (rightmost panels). * = significantly different from filtered air control; ~ = marginally different from filtered air control; n = 4/group

Fig. 4 Changes in correlation p values of Fe with other trace elements and metals following exposures to Fe only (left column) or Fe + SO$_2$ (right column) in lung, olfactory bulb and cortex (top, middle and bottom rows, respectively in females or males as indicated exposed to filtered air (A) or Fe or Fe + SO$_2$ (treated, T). * = significant correlation with Fe; n = 4/group

In olfactory bulb (Fig. 4 middle row), Fe was significantly correlated with Ca, S and Se in air-treated females in the Fe only exposure group, with all of these correlations eliminated post Fe only exposure. In air-exposed

males in the Fe only exposure group, correlations of Fe with Mg, P and S were found; Fe only exposure eliminated the correlations with Mg and P, while the correlation of Fe with S was retained, and a new correlation with

Sobolewski *et al. Particle and Fibre Toxicology*   (2022) 19:56

Page 8 of 19

Mn emerged. In contrast, following $Fe + SO_2$ exposures, an increase in Fe correlations with other metals was observed in females, that included emergence of correlations of Fe with Na, K, S and Se, while the correlation of Fe with Mn that was observed in air-treated females disappeared. Similarly, in air-treated males, Fe correlated only with Mn, but following the $Fe + SO_2$ exposure, new correlations of Fe emerged with Na, K, S and Se emerged, while the correlation with Mn disappeared.

The greatest number of increased correlations of Fe with other metals occurred following $Fe + SO_2$ exposures in cortex. In frontal cortex of air-exposed females (Fig. 4 bottom row), Fe was only associated with Mn, and this correlation was not evident in Fe only exposed females. In frontal cortex of air-treated males, Fe only exposure was initially correlated with Mg and Ca, while post Fe only exposure, the correlation of Fe with Mg was retained, and new correlations emerged between Fe with K and Zn. In the $Fe + SO_2$ exposure condition, Fe was initially associated with S and Se in the air-treated females, with $Fe + SO_2$ exposure further increasing correlations to include Fe with Mg, K, P, S, and Zn. While no correlations were seen in air-exposed males in the $Fe + SO_2$ exposure condition, here too the $Fe + SO_2$ exposure resulted in new correlations of Fe with Na, Mg, K, P, S, and Cu.

Figure 5 depicts the same data but for correlations of S with other metals/elements. In lung (top row) of

air-exposed females in the Fe only exposure condition, S was correlated with numerous other metals, including Na, Mg, K, Ca, P, Cu, Zn and Mn, and in the $Fe + SO_2$ exposure condition, S was correlated with Mg, K, P, Zn and Se in air-exposed females. With the exception of the correlation of S with K and P in the Fe only exposed group, these correlations disappeared following both Fe and $Fe + SO_2$ exposures. Air-treated males within the Fe only treatment group showed correlations of S with Mg, K, P and Zn, all of which were retained following Fe only exposure, and with new correlations of S with Na, Cu and Mn emerging. In contrast, in the $Fe + SO_2$ condition, S correlated with Na, Mg, K and Zn in air-treated males, but all of these correlations disappeared following $Fe + SO_2$ exposures.

Correlations of S with other metals/elements in olfactory bulb (middle row) of females were completely altered in the Fe only exposure condition, with initial correlations of S with Fe, Zn and Se in air-treated females, but altered to correlations of S with Na, Mg, K, P and Mn subsequent to Fe only exposure. Corresponding data in the $Fe + SO_2$ group revealed initial correlations of S with Mg, K, P and Cu in the air-exposed females, with Cu disappearing and Mn added following $Fe + SO_2$. In air-treated males within the Fe only exposed group, S was correlated with Mg, K and Fe, but correlations with Fe disappeared, while new correlations of S emerged with
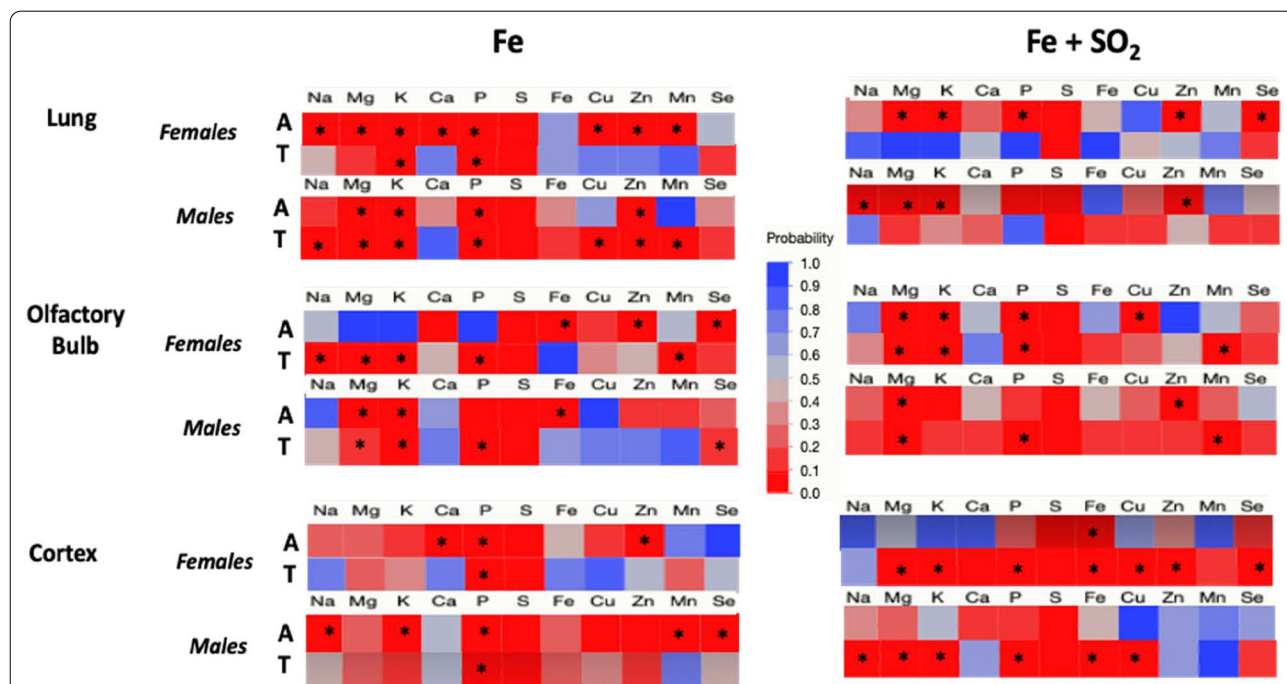
Fig. 5 Changes in correlation p values of S with other trace elements and metals following exposures to Fe only (left column) or $Fe + SO_2$ (right column) in lung, olfactory bulb and cortex (top, middle and bottom rows, respectively in females or males as indicated exposed to filtered air (A) or Fe or $Fe + SO_2$ (treated, T). * = significant correlation with S; n = 4/group

Sobolewski *et al. Particle and Fibre Toxicology*　　(2022) 19:56

Page 9 of 19

P and Se. In the $Fe + SO_2$ condition, S initially correlated with Mg and Zn in air-treated males, with the Zn correlation disappearing and new correlations with P and Mn emerging post combined Fe and SO_2 exposure.

$Fe + SO_2$, but not Fe only exposures, markedly increased correlations of S in female frontal cortex (bottom row), with correlations changing from Fe only to include Mg, K, P, Fe, Cu, Zn and Se following $Fe + SO_2$ exposure, whereas the correlations of S with Ca, P and Zn in air-treated females within the Fe only exposed group subsequently changed to a correlation only with P. In male frontal cortex, Fe only exposure eliminated correlations of S with Na, K, Mn and Se that were seen in air-treated males with only a correlation between S and P

retained. In contrast, an absence of correlations of S with other elements/metals was observed in the air-exposed male frontal cortex of the $Fe + SO_2$ group, with numerous correlations emerging post $Fe + SO_2$ exposure, including correlations of S with Na, Mg, K, P, Fe and Cu.

Brain neurotransmitter analyses

Levels of brain neurotransmitters in frontal cortex at PND14 are shown in Fig. 6 as percent of filtered air control values. For females, changes in frontal cortex in response to Fe only exposure or $Fe + SO_2$ exposures were limited, with the most marked effects being increases in dopamine turnover in response to Fe only, with significant increases in the ratios of both homovanillic (HVA)
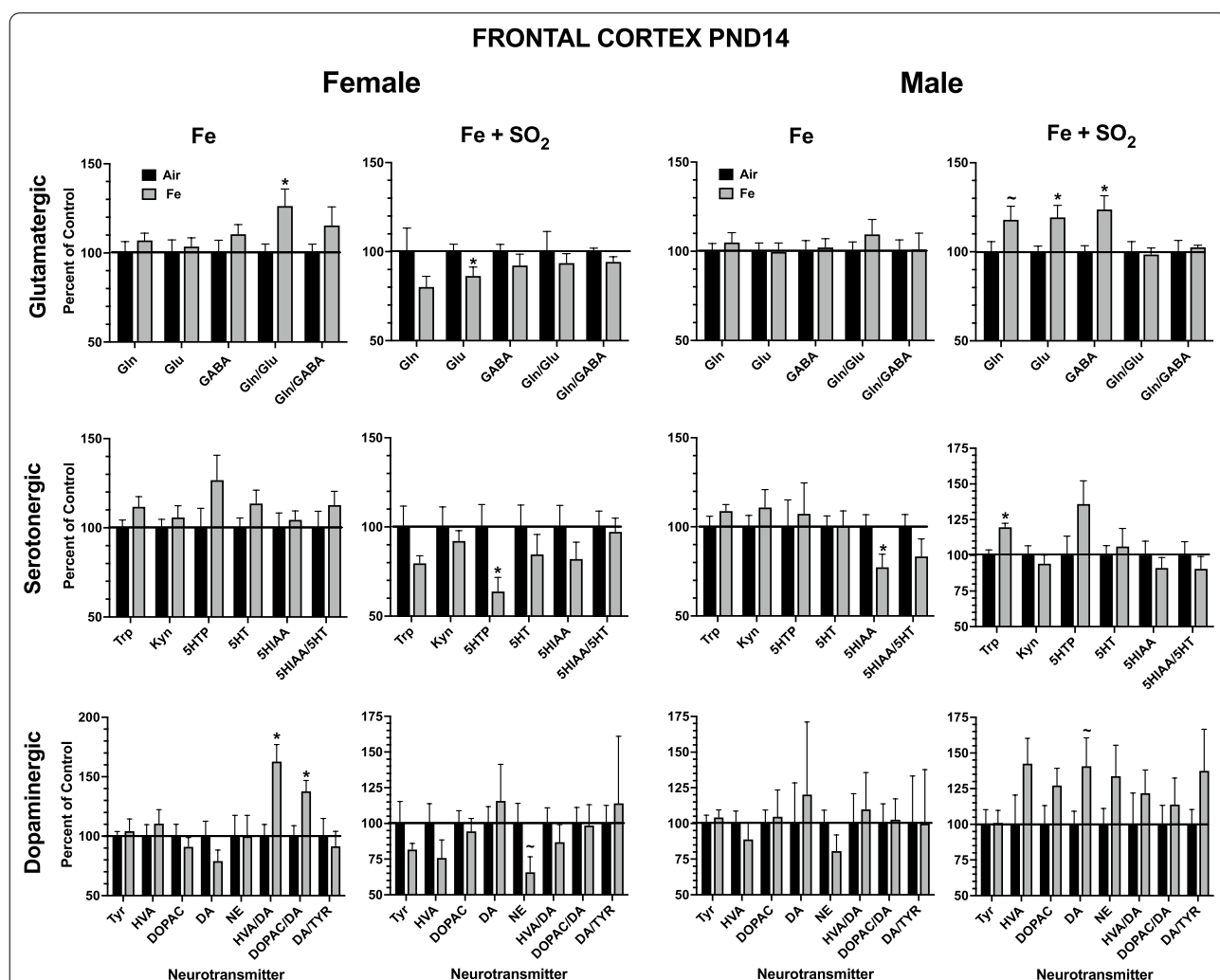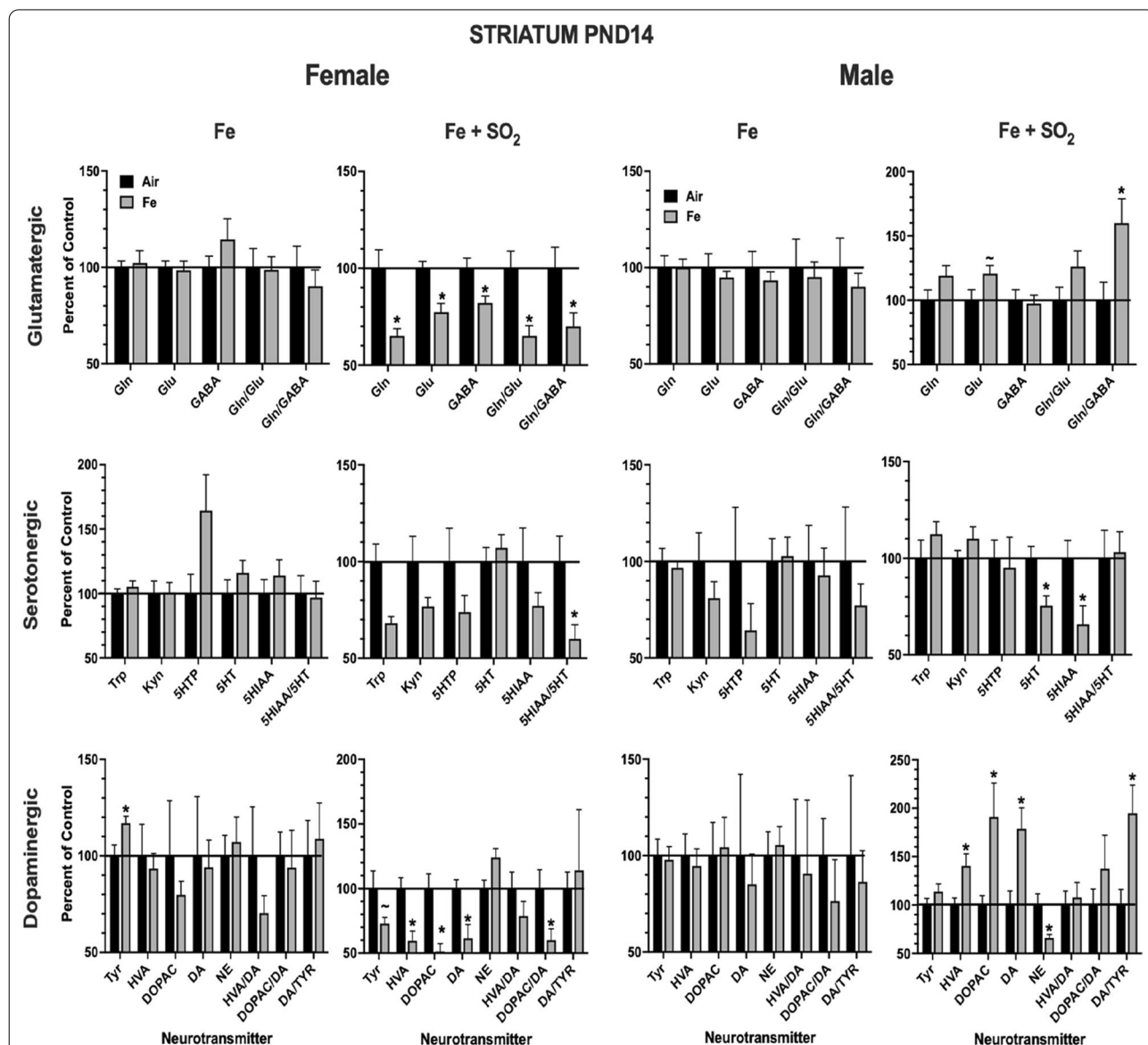

Fig. 6 Group mean ± S.E. percent change relative to filtered air control of frontal cortex neurotransmitter levels at PND14 in males and females exposed to Fe only or $Fe + SO_2$. * = significantly different from filtered air control; ~ = marginally different from filtered air control; n = 8/group. DA = dopamine; DOPAC = 3,4-dihydroxyphenylacetic acid; HVA = homovanillic acid, Tyr = tyrosine; NE = norepinephrine, Gln = glutamine; Glu = glutamate; GABA = gabba-aminobutyric acid; 5HT = serotonin; 5-HIAA = 5 hydroxyindoleacetic acid; 5-HTP = 5-hydroxytryptophan; Kyn = kynurenine; n = 7–8/group

Sobolewski *et al. Particle and Fibre Toxicology*   (2022) 19:56

Page 10 of 19

acid ($F(1,14) = 12.82$, $p = 0.003$) and of DOPAC to DA ($F(1,14) = 8.75$, $p = 0.01$). In males, the most notable effects were the significant increases in frontal cortical levels of glutamine ($F1,14) = 3.55$, $p = 0.0806$), glutamate ($F(1,14) = 6.56$, $p = 0.023$) and gamma aminobutyric acid (GABA; $F(1,14) = 8.11$, $p = 0.013$); trends consistent with increases in levels of dopaminergic neurotransmitters were found but were not significant.

Corresponding changes in striatum are presented in Fig. 7 and show that $Fe + SO_2$ exposure had far more impact in striatum in both sexes. For example, in females, marked reductions were seen in levels of glutamatergic neurotransmitters and turnover (glutamine ($F(1,18) = 11.68$, $p = 0.003$; glutamate ($F(1,18) = 15.76$, $p = 0/0.0009$; GABA ($F(1,18) = 7.94$, $p = 0.011$; glutamine/glutamate ($F(1,18) = 11.53$, $p = 0.003$; glutamate/GABA ($F(1,18) = 5.39$, $p = 0.032$), along with reductions in serotonin (5HT) turnover, i.e., 5 hydroxyindole acetic acid (5HIAA)/5HT ($F(1,18) = 7.12$, $p = 0.0156$), and in dopaminergic neurotransmitters and turnover

Fig. 7 Group mean ± S.E. percent change relative to filtered air control of striatal neurotransmitter levels at PND14 in males and females exposed to Fe only or Fe + SO₂. * = significantly different from filtered air control; ~ = marginally different from filtered air control; n = 8/group. DA = dopamine; DOPAC = 3,4-dihydroxyphenylacetic acid; HVA = homovanillic acid, Tyr = tyrosine; NE = norepinephrine, Gln = glutamine; Glu = glutamate; GABA = gabba-aminobutyric acid; 5HT = serotonin; 5-HIAA = 5 hydroxyindoleacetic acid; 5-HTP = 5-hydroxytryptophan; Kyn = kynurenine; n = 9–10/group

(tyrosine, F(1,18) = 3.52, $p = 0.077$; HVA (F(1,18) = 12.94, $p = 0.002$; DOPAC (F(1,18) = 14.36, $p = 0.001$; DA (F(1,18) = 9.3, $p = 0.007$; DOPAC/DA (F(1,18) = 5.55, $p = 0.03$). In the case of males, Fe + SO$_2$ exposure likewise reduced some serotonergic neurotransmitters, specifically 5HT F(1,17) = 9.49, $p = 0.007$) and 5 HIAA (F(1,17) = 6.64, $p = 0.02$), and, in contrast to females, markedly increased the dopaminergic neurotransmitters HVA (F(1,17) = 8.16, $p = 0.01$), DOPAC (F(1,17) = 6.95, $p = 0.017$) and DA (F(1,17) = 9.49, $p = 0.007$) and DA/ tyrosine (F(1,17) = 8.56, $p = 0.009$), while reducing levels of norepinephrine (NE) (F(1,17) = 7.3, $p = 0.015$).

By PND60, few and predominately marginal changes in frontal cortex were seen in females (Additional file 1: Fig. 1), while males primarily showed marginal reductions in serotonin and its metabolite 5HIAA and turnover in response to Fe only exposures. Similarly, significant changes in striatal neurotransmitters were not apparent at PND60 (Additional file 1: Fig. 2), with the exception in females of increases in 5HT turnover after Fe only (F(1,14) = 5.16, $p = 0.039$) and of DA turnover (DOPACC/DA, F(1,13) = 7.01, $p = 0.02$) in response to Fe + SO$_2$ exposure.

Inflammation and oxidative stress

Frontal Cortex Trans-Sulfuration Markers—Several markers of the trans-sulfuration pathway were assessed in frontal cortex and are plotted as percent of control in Fig. 8. As it shows, significant changes in this pathway were seen only after Fe + SO$_2$ at PND14. Specifically, these included significant reductions in homocysteine F(1,14) = 7.66, $p = 0.015$) and marginal increases in cysteine (F(1,14) = 3.91, $p = 0.068$) in females, and significant increases in methionine (F(1,14) = 10.67, $p = 0.006$) and marginal increases in homocysteine (F(1,14) = 3.66, $p = 0.077$) in males. The only significant change were increases in cysteine in males in response to Fe only at PND60.

Serum Glutathione (GSH)—Serum levels of glutathione were selectively increased in females in response to Fe + SO$_2$ exposure (Fig. 9, left panel) by approximately 38%, an effect that just missed statistical significance (F(1,22) = 4.01, $p = 0.0576$). No effects were seen in response to Fe + SO$_2$ exposure in males, nor did Fe only alter serum GSH in either sex.
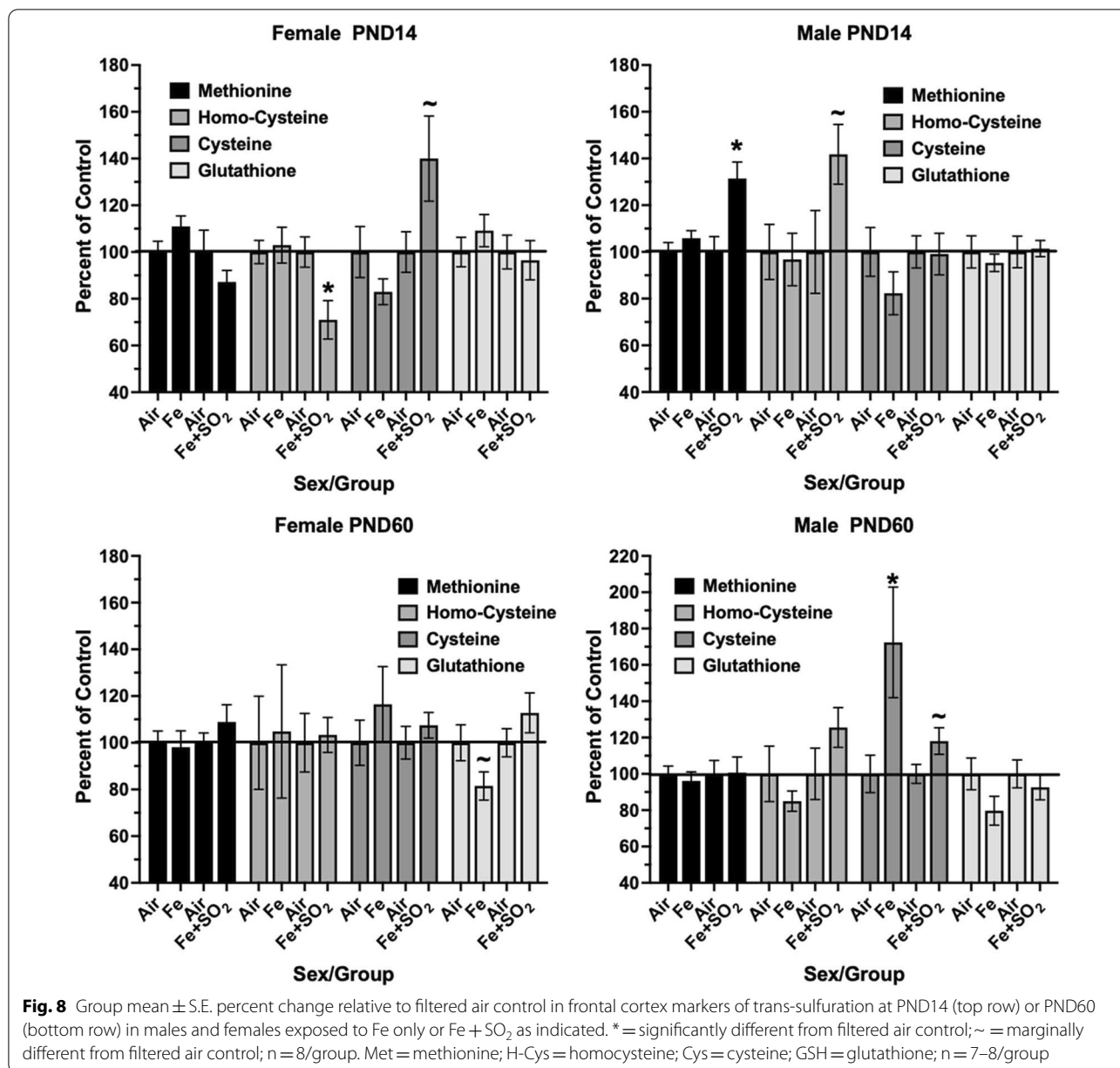
Cytokines—Levels of IL-1a in serum were the only detectable cytokines at PND14 and are shown in Fig. 9, right panel. As it shows, increases in females in mean levels of IL-1a (F(1,10) = 6.06, $p = 0.034$) were found after Fe + SO$_2$ exposure, with similar but non-significant trends in response to Fe only in males. Exposures to Fe + SO$_2$ did not produce changes in IL-1a in males.

Discussion

This study sought to determine whether Fe as a contaminant of air pollution exposures would reproduce features previously seen in response to postnatal and/or gestational ambient ultrafine particle exposures of mice. Brain Fe overload can result in oxidative stress and ferroptosis [79, 80], and the brain has no apparent mechanisms to excrete Fe to the periphery [81, 82]. Two general findings emerged from this study. First, comparisons of the number and magnitude of effects indicate a greater overall toxicity of Fe + SO$_2$ as compared to Fe only exposures (Table 1) in both sexes, as shown by a broader set of changes in correlations of Fe + SO$_2$ with other metals and trace elements, and in neurotransmitter changes at postnatal day 14, as well as female specific changes in serum GSH and the inflammatory cytokine, IL-1a. Such findings suggest that the chemical mixture clearly matters. The greater effects of Fe + SO$_2$ may be consistent with reports that sulfide can produce acidic aerosols that can dissolve transition metals [83, 84], and other studies reporting that SO$_2$ increased uptake of Fe$_2$O$_3$ in mouse bronchial epithelium and altered its intracellular distribution [66].

Another observation is an apparent greater vulnerability of females than males to Fe and Fe + SO$_2$ exposures, based on the selective effects in females in body weight, GSH and IL-1a, and in frontal cortex metal level changes following Fe only. Sex differences in brain Fe levels and differences in Fe homeostasis have been reported in humans and in animal models. For example, human females have been reported to have lower levels of the Fe export protein ferritin in brain than do males [85], while another study reported lower total subcortical brain Fe in women from midlife relative to men and to younger women [86]. Interestingly, differences in Fe status are seen even during infancy [87]. Nevertheless, an understanding of sex differences in early Fe handling and function and its impact on brain development is lacking.
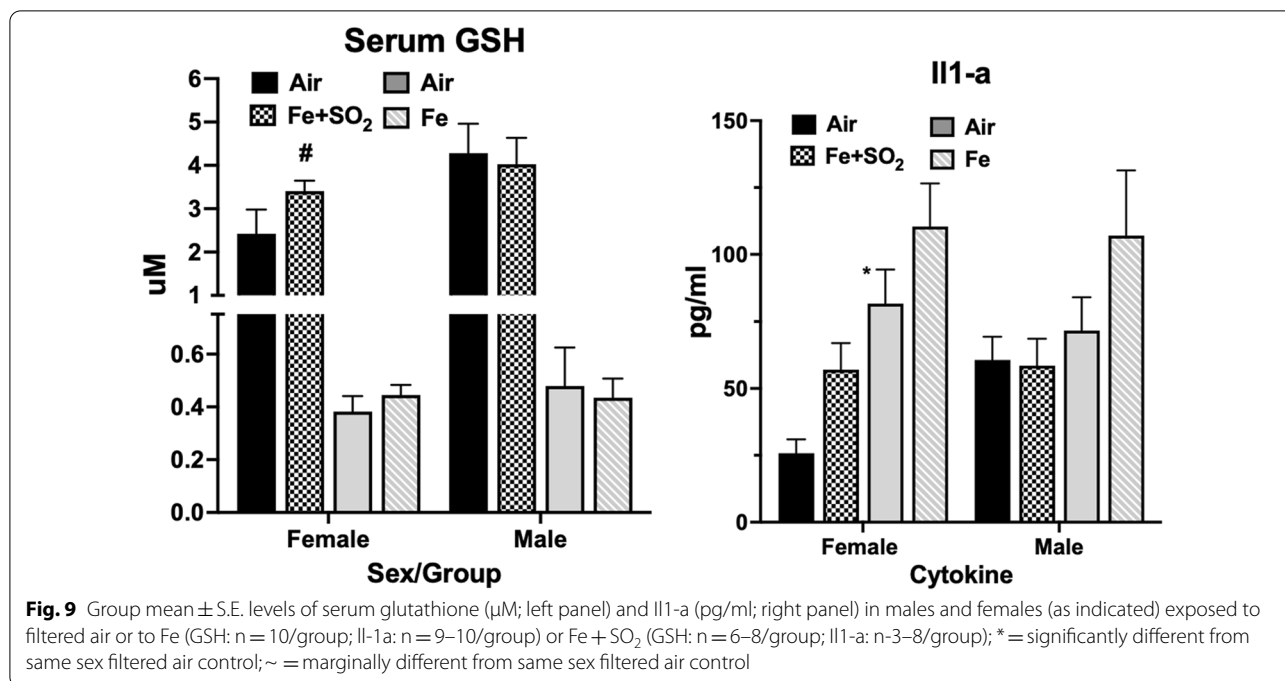
Metal dyshomeostasis was found after both Fe only and Fe + SO$_2$ exposures in both sexes as evidenced not only by altered levels of metals in lung and brain, but additionally as seen in alterations in correlations of both Fe and S with other metals/elements within these regions, which was particularly striking in frontal cortex. Metal dyshomeostasis has been implicated in neurodevelopmental disorders [52–55] as well as in neurodegenerative diseases and disorders [88, 89]. Here too, both sex and chemical mixture contributed to differences in outcome. For example, in frontal cortex, Fe only exposure reduced levels of multiple metals/trace elements in females, with no such effects observed in response to Fe + SO$_2$; in contrast, males showed increases in several metals/elements in frontal cortex following Fe + SO$_2$ exposure, whereas Fe alone had no effect. Further, increases in levels of Fe were

Sobolewski *et al. Particle and Fibre Toxicology*   (2022) 19:56

Page 12 of 19

Fig. 8 Group mean ± S.E. percent change relative to filtered air control in frontal cortex markers of trans-sulfuration at PND14 (top row) or PND60 (bottom row) in males and females exposed to Fe only or Fe + SO₂ as indicated. * = significantly different from filtered air control; ~ = marginally different from filtered air control; n = 8/group. Met = methionine; H-Cys = homocysteine; Cys = cysteine; GSH = glutathione; n = 7–8/group

marginal in female lung after Fe only exposure, but significant in males after Fe + SO₂ exposures.

Multiple neurochemical changes were seen in response to ambient UFP exposures in both frontal cortex and striatum of mice in our prior studies of exposures to concentrated ambient UFPs [68]. Similarly, neurochemical changes were observed in the current study. These included changes in dopaminergic function, particularly in striatum in response to Fe + SO₂ exposures, again with effects that were of opposite direction by sex, with reductions seen in females, whereas increases occurred in males. Similarly, our

prior studies of ambient UFPs have revealed evidence of sex specific changes in dopaminergic function, including alterations at postnatal days 14 and 55 [14] and at PND270 [68]. Sex differences in DA function and corresponding consequences have long been known, including in human studies [90]. Reports in rats include enhanced DA release in female rats [91], and of maximal velocity of DA reuptake in females [92] as compared to males. One suggested basis for such differences has been a greater DA terminal density in females compared to males in caudate nucleus [92]. Males were reported to show a greater overproduction of striatal

Fig. 9 Group mean ± S.E. levels of serum glutathione (μM; left panel) and Il1-a (pg/ml; right panel) in males and females (as indicated) exposed to filtered air or to Fe (GSH: n = 10/group; ll-1a: n = 9–10/group) or Fe + SO₂ (GSH: n = 6–8/group; ll1-a: n-3–8/group); * = significantly different from same sex filtered air control; ~ = marginally different from same sex filtered air control

Table 1 Summary of Changes in Response to Fe Only or to Combined Fe + SO$_2$

	Females		Males	
	Fe	Fe + SO₂	Fe	Fe + SO₂
Body weight		↓		
Lung metal	↓P	↓Mn	↑Ca, Na	↑Fe
Olfactory Bulb matals	↑Zn	↓K		
Frontal cortex metals	↓Mg, K, Ca, P, S, Cu, Zn			↑Mg, K, Zn
Lung Fe correlations	Na	Mg, P	Zn	
Olfactory bulb Fe correlations	Ca, S, Se	Na, K, S, Mn, SE	Mg, P, Mn	Na, K, S, Mn, Se
Frontal cortex Fe correlations	Mn	Mg, K, P, Zn, Se	K, Ca, Zn	Na, Mg, K, P, S, Cu
Lung Fe correlations	Na, Mg, Ca, Cu, Mn	Mg, K, P, Zn, Se	Na, Cu, Mn	Na, Mg, K, Zn
Olfactory bulb S correlations	Na, Mg, K, P, Fe, Zn, Mn, Se	Cu, Mn	P, Fe, Se	P, Zn, Mn
Frontal cortex S correlations	Ca, Zn	↓Mg, K, P, Cu, Zn, Se	Na, K, Mn, Se	Na, Mg, K, P, Fe, Cu
Frontal cortex Glutamatergic PND14	↑Gln/Glu	↓Glu		~ ↑Gln, ↑Glu, GABA
Frontal cortex Serotonergic PND14		↓5HTP	↓5HIAA	↑Trp
Frontal cortex Dopaminergic PND14	↑HVA/DA, DOPAC/DA	~ ↓NE		~ ↑DA
Striatal Glutamatergic PND14		↓Gln, Glu, GABA, Gln/Glu, Glu/GABA		~ ↑Glu, ↑Glu/ GABA
Striatal Serotonergic PND14		↓5HIAA/5HT		↓5HIAA, 5HT
Striatal Dopaminergic PND14	↑Tyr	~ ↓Tyr, ↓HVA, DOPAC, DA, D		↑HVA, DOPADA, DA/Tyr, ↓NE
Frontal Cortex Trans-Sulfuration PND14		↓H-Cys, ~ ↑Cys	~ ↑Cys	↑Met, ~ ↑H-Cys
Serum Glutathione		~ ↑		
Serum IL1a		↑		
Lateral Ventricle area	↑	↓		
Lateral Ventricle perimeter	↑	↑		

Summary of changes in response to Fe only or combined Fe + SO₂. ↑, significant increase; ↓, significant decrease; ~ , marginally significant; DA, Dopamine; DOPAC, 3,4-dihydroxyphenylacetic acid; HVA, Homovanillic acid; Tyr, Tyrosine; NE, Norepinephrine; Gln, Glutamine; Glu, Glutamate; GABA, Gabba-aminobutyric acid; 5HT, Serotonin; 5-HIAA, 5 hydroxyindoleacetic acid; 5-HTP, 5-hydroxytryptophan; Kyn, Kynurenine; Met, Methionine; H-Cys, Homocysteine; Cys, Cysteine; GSH, Glutathione

Sobolewski *et al. Particle and Fibre Toxicology*   (2022) 19:56

Page 14 of 19

D1 and D2 receptors in comparison to females [93]. A potential role for Fe contamination of UFPs in DA changes is highly plausible, as DA metabolism can produce neurotoxic species, particularly quinones which can then form neurotoxic intermediates via Fe-dependent reactions [94]. DA can also increase uptake of labile Fe by macrophages resulting in oxidative stress [95]. In addition, DA quinones can react with S-containing compounds such as l-cysteine and reduced glutathione tripeptide, both of which are present in high concentrations in brains, ultimately leading to toxic produces such as 5-S-Cys-dopamine that can lead to DA neuronal death [96].

Of particular note in the current study, increases in frontal cortex glutamine, glutamate and GABA and of striatal glutamate and glutamate/GABA were seen in males in response to $Fe + SO_2$. Such findings are consistent with those produced by developmental exposures to ambient UFPs in our prior studies of increases in males observed at both PND14 and PND55 [14] following UFP exposures with a mean of 96 ug/m^3. Such findings are reminiscent of excitatory/inhibitory imbalance, considered a key feature of autism and schizophrenia [97]. Again, however, consistent with sex differences in response to Fe, $Fe + SO_2$ decreased glutamate in females, whereas increases in glutamate turnover occurred in response to Fe only in females. Sex- and brain-region related differences in levels of glutamate, GABA and aspartate have previously been documented, and include differences seen in the early postnatal period in rat brain [98]. In juvenile rats, for example, GLU signaling molecules were found at significantly lower levels in females [99]. Sex differences in GLU function are likewise reported in humans, and have included more rapid age-related declines in glutamate in males [100]. Collectively, such findings suggest a role for Fe in the persistence of UFP-induced excitatory/inhibitory imbalance we previously observed seen in males; importantly this is considered a key feature of autism and schizophrenia [97], both of which are male-biased disorders.

Mechanistically, glutamate has the potential for neurotoxic interactions with Fe, specifically in the framework of ferroptosis, wherein glutamate can inhibit uptake of cystine by the cystine/glutamate antiporter resulting in glutathione depletion, thereby facilitating Fe-produced oxidative damage [101, 102]. The glutamine-glutamate cycle is within the brain's trans-sulfuration pathway [103, 104]. Notably, a recent study suggested a stronger regulatory control between peripheral Fe and glutamate metabolism in females [105].

The trans-sulfuration pathway is also well known to interact with glutamatergic systems and functions [106–108] and thus it is possible that elevations in frontal cortex glutamate seen in males, and reductions in glutamate seen in females in response to $Fe + SO_2$ could be due to oxidative stress-related effects of Fe. However, changes in trans-sulfuration systems appear to occur in a sex-dependent capacity and can be influenced by hormones [109–112]. Such sex differences were reflected in the profiles of both trans-sulfuration markers and glutamatergic changes seen in response to $Fe + SO_2$ in this study (Fig. 10). Correspondingly, these findings suggest that mechanistic links between these systems, and thus ultimately, mechanistic links both in excitotoxicity and redox status, and their direction of causation, will likely differ by sex.

Interestingly, although our previous research on postnatal exposure conducted in Rochester, NY shows strong male-biased early toxicity to concentrated ambient ultrafine particles, our previous work on gestational exposures conducted in Sterling, NY shows significant female and male effects. These gestational exposures, however, as carried out in Sterling NY were more enriched with Fe as measured by Elemental X-Ray Fluorescence, with Fe levels indicating a 376 fold increase over filtered air (FA). Average Fe concentrations on filters from filtered air chambers were 3.8 ng/m^3, while exposure filter values were 1,430 ng/m^3 [18, 19, 113]. Future research is needed to explore the sex-dependent effect of Fe exposure in early gestation as compared to postnatal exposures.

Given that the ambient exposures include numerous metals and organics as a mixture, and thus exposures to Fe only would not be expected to fully or explicitly reproduce all of the neurotoxic effects of ambient air pollution, the current evidence suggests that Fe contamination of UFP does contribute to features of the neurotoxicity of ambient air pollution, with different impacts by sex and outcome measures. It should also be noted that the exposures used here produced a consistently high number concentration exposure of pure Fe particles, exceeding what would be seen in Fe ambient environmental exposure levels by number. Nevertheless, an increased understanding of the role of metal contaminants in air pollution as a contributor to the etiology of neurodevelopmental disorders and neurodegenerative diseases is critical given that these are life-long exposures beginning in utero. Such an understanding can guide the development of more realistic focused animal exposure models of human AP exposure as well as allow refinement of epidemiological studies, and, consequently, a more meaningful approach to mechanistic studies. In addition, it would be potentially informative in population studies, for example, using geographic mapping of exposures to various metal contaminants of AP, along with gases such as SO_2, where available, in relation to diagnostic or

Sobolewski *et al. Particle and Fibre Toxicology*   (2022) 19:56

Page 15 of 19
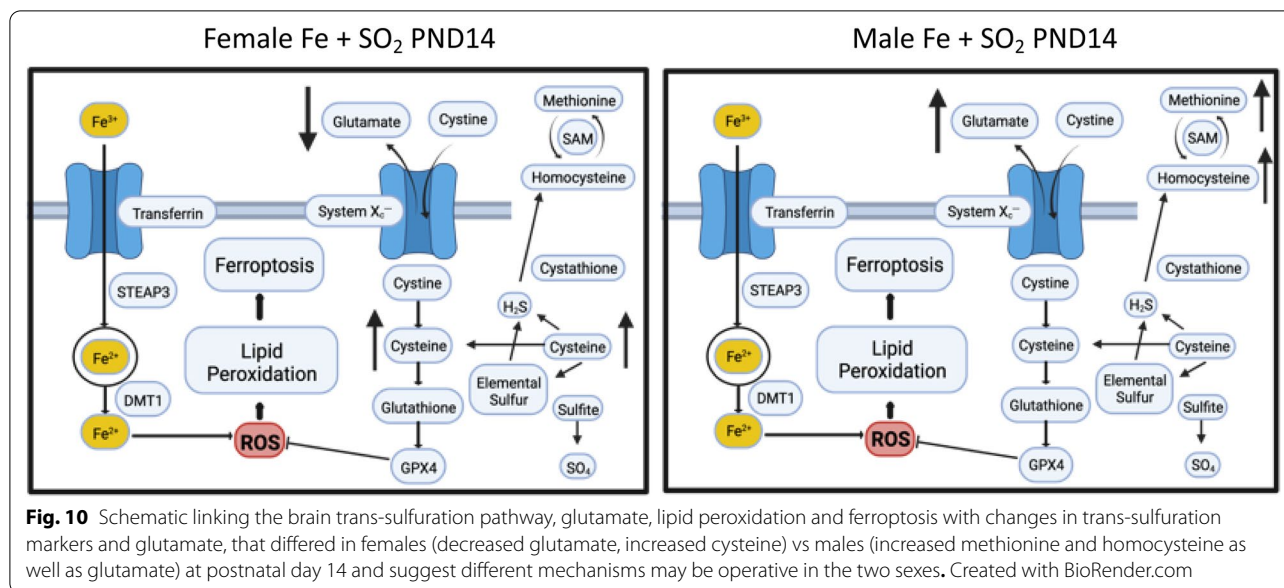
Fig. 10 Schematic linking the brain trans-sulfuration pathway, glutamate, lipid peroxidation and ferroptosis with changes in trans-sulfuration markers and glutamate, that differed in females (decreased glutamate, increased cysteine) vs males (increased methionine and homocysteine as well as glutamate) at postnatal day 14 and suggest different mechanisms may be operative in the two sexes. Created with BioRender.com

incidence data for various neurodevelopmental disorders and neurodegenerative diseases [30]. Such studies would also point to potential intervention strategies for neurodevelopmental disorders and neurodegenerative diseases. Understanding the components of AP relating to neurotoxicity is of direct translational relevance to public health protection, as it can provide information pertinent to regulations of exposures, including the need for new or more stringent regulations.

Supplementary Information

The online version contains supplementary material available at https://doi.org/10.1186/s12989-022-00496-5.

Additional file 1. Supplemental Figure 1: Group mean ± S.E. percent change relative to filtered air control of frontal cortex neurotransmitter levels at PND60 in males and females exposed to Fe only or Fe + SO$_2$. *= significantly different from filtered air control; ~=marginally different from filtered air control; n=8/group. DA=dopamine; DOPAC=3,4-dihydroxyphenylacetic acid; HVA=homovanillic acid, Tyr=tyrosine; NE=norepinephrine, Gln=glutamine; Glu=glutamate; GABA=gabba-aminobutyric acid; 5HT=serotonin; 5-HIAA=5 hydroxyindoleacetic acid; 5-HTP=5-hydroxytryptophan; Kyn=kynurenine; n=7-8/group.
Supplemental Figure 2: Group mean ± S.E. percent change relative to filtered air control of striatal neurotransmitter levels at PND60 in males and females exposed to Fe only or Fe + SO$_2$. *= significantly different from filtered air control; ~=marginally different from filtered air control; n=8/group. DA=dopamine; DOPAC=3,4-dihydroxyphenylacetic acid; HVA=homovanillic acid, Tyr=tyrosine; NE=norepinephrine, Gln=glutamine; Glu=glutamate; GABA=gabba-aminobutyric acid; 5HT=serotonin; 5-HIAA=5 hydroxyindoleacetic acid; 5-HTP=5-hydroxytryptophan; Kyn=kynurenine; n=9-10/group.

Availability of data and materials
The datasets used and/or analyzed in the current study are available from the corresponding author on reasonable request.

Declarations

Ethics approval and consent to participate
This study was carried out in accordance with relevant guidelines and regulations. All mice were used and treated via protocols approved by the University of Rochester Medical Center Institutional Animal Care and Use Committee and Committee on Animal Resources (approval # 102208 / 2010-046E), and in accordance with NIH guidelines.

Consent for publication
Not applicable.

Competing interests
The authors declare that they have no competing interests.

Author details
[1]Department of Environmental Medicine, University of Rochester Medical Center, Rochester, NY 14642, USA. [2]Department of Psychology, Radford University, Radford, VA 24142, USA. [3]Proteomics Core, University of Rochester Medical Center, Rochester, NY 14642, USA. [4]Department of Earth Sciences, Dartmouth College, Hanover, NH 03755, USA.

Sobolewski *et al. Particle and Fibre Toxicology*   (2022) 19:56

Page 16 of 19

References

1. Attademo L, Bernardini F. Air pollution as risk factor for mental disorders: in search for a possible link with Alzheimer's disease and schizophrenia. J Alzheimers Dis. 2020;76(3):825–30. https://doi.org/10.3233/jad-200289.
2. Babadjouni RM, Hodis DM, Radwanski R, Durazo R, Patel A, Liu Q, et al. Clinical effects of air pollution on the central nervous system; a review. J Clin Neurosci. 2017;43:16–24. https://doi.org/10.1016/j.jocn.2017.04.028.
3. Costa LG, Cole TB, Dao K, Chang YC, Coburn J, Garrick JM. Effects of air pollution on the nervous system and its possible role in neurodevelopmental and neurodegenerative disorders. Pharmacol Ther. 2020;210:107523. https://doi.org/10.1016/j.pharmthera.2020.107523.
4. Chun H, Leung C, Wen SW, McDonald J, Shin HH. Maternal exposure to air pollution and risk of autism in children: a systematic review and meta-analysis. Environ Pollut. 2020;256:113307. https://doi.org/10.1016/j.envpol.2019.113307.
5. McGuinn LA, Windham GC, Kalkbrenner AE, Bradley C, Di Q, Croen LA, et al. Early life exposure to air pollution and autism spectrum disorder: findings from a multisite case-control study. Epidemiology. 2020;31(1):103–14. https://doi.org/10.1097/ede.0000000000001109.
6. Oudin A, Frondelius K, Haglund N, Källén K, Forsberg B, Gustafsson P, et al. Prenatal exposure to air pollution as a potential risk factor for autism and ADHD. Environ Int. 2019;133:105149. https://doi.org/10.1016/j.envint.2019.105149.
7. Volk HE, Lurmann F, Penfold B, Hertz-Picciotto I, McConnell R. Traffic-related air pollution, particulate matter, and autism. JAMA Psychiat. 2013;70(1):71–7. https://doi.org/10.1001/jamapsychiatry.2013.266.
8. Antonsen S, Mok PLH, Webb RT, Mortensen PB, McGrath JJ, Agerbo E, et al. Exposure to air pollution during childhood and risk of developing schizophrenia: a national cohort study. Lancet Planet Health. 2020;4(2):e64–73. https://doi.org/10.1016/s2542-5196(20)30004-8.
9. Worthington MA, Petkova E, Freudenreich O, Cather C, Holt D, Bello I, et al. Air pollution and hippocampal atrophy in first episode schizophrenia. Schizophr Res. 2020;218:63–9. https://doi.org/10.1016/j.schres.2020.03.001.
10. Clancy B, Finlay BL, Darlington RB, Anand KJ. Extrapolating brain development from experimental species to humans. Neurotoxicology. 2007;28(5):931–7. https://doi.org/10.1016/j.neuro.2007.01.014.
11. Clancy B, Kersh B, Hyde J, Darlington RB, Anand KJ, Finlay BL. Web-based method for translating neurodevelopment from laboratory species to humans. Neuroinformatics. 2007;5(1):79–94.
12. Allen JL, Conrad K, Oberdorster G, Johnston CJ, Sleezer B, Cory-Slechta DA. Developmental exposure to concentrated ambient particles and preference for immediate reward in mice. Environ Health Perspect. 2013;121(1):32–8. https://doi.org/10.1289/ehp.1205505.
13. Allen JL, Klocke C, Morris-Schaffer K, Conrad K, Sobolewski M, Cory-Slechta DA. Cognitive effects of air pollution exposures and potential mechanistic underpinnings. Curr Environ Health Rep. 2017;4(2):180–91. https://doi.org/10.1007/s40572-017-0134-3.
14. Allen JL, Liu X, Pelkowski S, Palmer B, Conrad K, Oberdorster G, et al. Early postnatal exposure to ultrafine particulate matter air pollution: persistent ventriculomegaly, neurochemical disruption, and glial activation preferentially in male mice. Environ Health Perspect. 2014;122(9):939–45. https://doi.org/10.1289/ehp.1307984.
15. Allen JL, Oberdorster G, Morris-Schaffer K, Wong C, Klocke C, Sobolewski M, et al. Developmental neurotoxicity of inhaled ambient ultrafine particle air pollution: parallels with neuropathological and behavioral features of autism and other neurodevelopmental disorders. Neurotoxicology. 2015. https://doi.org/10.1016/j.neuro.2015.12.014.
16. Sobolewski M, Anderson T, Conrad K, Marvin E, Klocke C, Morris-Schaffer K, et al. Developmental exposures to ultrafine particle air pollution reduces early testosterone levels and adult male social novelty preference: risk for children's sex-biased neurobehavioral disorders. Neurotoxicology. 2018;68:203–11. https://doi.org/10.1016/j.neuro.2018.08.009.
17. Klocke C, Allen JL, Sobolewski M, Blum JL, Zelikoff JT, Cory-Slechta DA. Exposure to fine and ultrafine particulate matter during gestation alters postnatal oligodendrocyte maturation, proliferation capacity, and myelination. Neurotoxicology. 2018;65:196–206. https://doi.org/10.1016/j.neuro.2017.10.004.
18. Klocke C, Allen JL, Sobolewski M, Mayer-Pröschel M, Blum JL, Lauterstein D, et al. Neuropathological consequences of gestational exposure to concentrated ambient fine and ultrafine particles in the mouse. Toxicol Sci. 2017;156(2):492–508. https://doi.org/10.1093/toxsci/kfx010.
19. Klocke C, Sherina V, Graham UM, Gunderson J, Allen JL, Sobolewski M, et al. Enhanced cerebellar myelination with concomitant iron elevation and ultrastructural irregularities following prenatal exposure to ambient particulate matter in the mouse. Inhal Toxicol. 2018;30(9–10):381–96. https://doi.org/10.1080/08958378.2018.1533053.
20. Richards R, Greimel E, Kliemann D, Koerte IK, Schulte-Körne G, Reuter M, et al. Increased hippocampal shape asymmetry and volumetric ventricular asymmetry in autism spectrum disorder. Neuroimage Clin. 2020;26:102207. https://doi.org/10.1016/j.nicl.2020.102207.
21. Turner AH, Greenspan KS, van Erp TGM. Pallidum and lateral ventricle volume enlargement in autism spectrum disorder. Psychiatry Res Neuroimaging. 2016;252:40–5. https://doi.org/10.1016/j.pscychresns.2016.04.003.
22. Cuesta MJ, Lecumberri P, Cabada T, Moreno-Izco L, Ribeiro M, Lopez-Ilundain JM, et al. Basal ganglia and ventricle volume in first-episode psychosis. A family and clinical study. Psychiatry Res Neuroimaging. 2017;269:90–6. https://doi.org/10.1016/j.pscychresns.2017.09.010.
23. Verkhlyutov VM, Gapienko GV, Ushakov VL, Portnova GV, Verkhlyutova IA, Anisimov NV, et al. MRI morphometry of the cerebral ventricles in patients with attention deficit hyperactivity disorder. Neurosci Behav Physiol. 2010;40(3):295–303. https://doi.org/10.1007/s11055-010-9256-x.
24. Milovanovic N, Damjanovic A, Puskas L, Milovanovic S, Barisic J, Malis M, et al. Reliability of the bicaudate parameter in the revealing of the enlarged lateral Ventricles in schizophrenia patients. Psychiatr Danub. 2018;30(2):150–6. https://doi.org/10.24869/psyd.2018.150.
25. Blackmon K, Ben-Avi E, Wang X, Pardoe HR, Di Martino A, Halgren E, et al. Periventricular white matter abnormalities and restricted repetitive behavior in autism spectrum disorder. NeuroImage Clin. 2016;10:36–45. https://doi.org/10.1016/j.nicl.2015.10.017.
26. Yang M, Gao S, Zhang X. Cognitive deficits and white matter abnormalities in never-treated first-episode schizophrenia. Transl Psychiatry. 2020;10(1):368. https://doi.org/10.1038/s41398-020-01049-0.
27. Wu ZM, Llera A, Hoogman M, Cao QJ, Zwiers MP, Bralten J, et al. Linked anatomical and functional brain alterations in children with attention-deficit/hyperactivity disorder. Neuroimage Clin. 2019;23:101851. https://doi.org/10.1016/j.nicl.2019.101851.
28. Hu W, MacDonald ML, Elswick DE, Sweet RA. The glutamate hypothesis of schizophrenia: evidence from human brain tissue studies. Ann N Y Acad Sci. 2015;1338:38–57. https://doi.org/10.1111/nyas.12547.
29. Bauer J, Werner A, Kohl W, Kugel H, Shushakova A, Pedersen A, et al. Hyperactivity and impulsivity in adult attention-deficit/hyperactivity disorder is related to glutamatergic dysfunction in the anterior cingulate cortex. World J Biol Psychiatry. 2016. https://doi.org/10.1080/15622975.2016.1262060.
30. Cory-Slechta DA, Sobolewski M, Oberdörster G. Air pollution-related brain metal dyshomeostasis as a potential risk factor for neurodevelopmental disorders and neurodegenerative diseases. Atmosphere. 2020;11(10):1098.
31. Ault AP, Peters TM, Sawvel EJ, Casuccio GS, Willis RD, Norris GA, et al. Single-particle SEM-EDX analysis of iron-containing coarse particulate matter in an urban environment: sources and distribution of iron within Cleveland. Ohio Environ Sci Technol. 2012;46(8):4331–9. https://doi.org/10.1021/es204006k.
32. Luglio David G, Katsigeorgis M, Hess J, Kim R, Adragna J, Raja A, et al. PM2.5 concentration and composition in subway systems in the northeastern United States. Environ Health Perspect. 2021;129(2):27001. https://doi.org/10.1289/EHP7202.
33. Chen R, Cheng J, Lv J, Wu L, Wu J. Comparison of chemical compositions in air particulate matter during summer and winter in Beijing, China. Environ Geochem Health. 2017;39(4):913–21. https://doi.org/10.1007/s10653-016-9862-9.
34. Bem H, Gallorini M, Rizzio E, Krzemińska M. Comparative studies on the concentrations of some elements in the urban air particulate matter in Lodz City of Poland and in Milan, Italy. Environ Int. 2003;29(4):423–8. https://doi.org/10.1016/S0160-4120(02)00190-3.

Sobolewski *et al. Particle and Fibre Toxicology*   (2022) 19:56

Page 17 of 19

35. Mansha M, Ghauri B, Rahman S, Amman A. Characterization and source apportionment of ambient air particulate matter (PM2.5) in Karachi. Sci Total Environ. 2012;425:176–83. https://doi.org/10.1016/j.scitotenv.2011.10.056.

36. Reff A, Bhave PV, Simon H, Pace TG, Pouliot GA, Mobley JD, et al. Emissions inventory of PM2.5 trace elements across the United States. Environ Sci Technol. 2009;43(15):5790–6. https://doi.org/10.1021/es802930x.

37. Cerami C. Iron nutriture of the fetus, neonate, infant, and child. Ann Nutr Metab. 2017;71(Suppl 3):8–14. https://doi.org/10.1159/000481447.

38. Georgieff MK. Iron assessment to protect the developing brain. Am J Clin Nutr. 2017;106(Suppl 6):1588s-s1593. https://doi.org/10.3945/ajcn.117.155846.

39. Lozoff B, Georgieff MK. Iron deficiency and brain development. Semin Pediatr Neurol. 2006;13(3):158–65. https://doi.org/10.1016/j.spen.2006.08.004.

40. Raffaeli G, Manzoni F, Cortesi V, Cavallaro G, Mosca F, Ghirardello S. Iron homeostasis disruption and oxidative stress in preterm newborns. Nutrients. 2020. https://doi.org/10.3390/nu12061554.

41. Rassin DK, Sturman JA, Gaull GE. Sulfur amino acid metabolism in the developing rhesus monkey brain: subcellular studies of taurine, cysteinesulfinic acid decarboxylase, gamma-aminobutyric acid, and glutamic acid decarboxylase. J Neurochem. 1981;37(3):740–8. https://doi.org/10.1111/j.1471-4159.1982.tb12550.x.

42. Rassin DK, Sturman JA, Gaull GE. Sulfur amino acid metabolism in the developing rhesus monkey brain: subcellular studies of the methylation cycle and cystathionine beta-synthase. J Neurochem. 1981;36(3):1263–71. https://doi.org/10.1111/j.1471-4159.1981.tb01726.x.

43. Stipanuk MH, Ueki I. Dealing with methionine/homocysteine sulfur: cysteine metabolism to taurine and inorganic sulfur. J Inherit Metab Dis. 2011;34(1):17–32. https://doi.org/10.1007/s10545-009-9006-9.

44. Adachi T, Yasutake A, Hirayama K. Influence of dietary levels of protein and sulfur amino acids on metabolism of glutathione and related amino acids in mice. J Health Sci. 2002;48(5):446–50. https://doi.org/10.1248/jhs.48.446.

45. Olkowski AA, Gooneratne SR, Crichlow EC, Rousseaux CG, Christensen DA. Effects of high dietary sulfur on brain functions using evoked-potentials technique. Can J Vet Res. 1990;54(1):113–8.

46. Brissot P, Troadec MB, Loréal O, Brissot E. Pathophysiology and classification of iron overload diseases; update 2018. Transfus Clin Biol. 2019;26(1):80–8. https://doi.org/10.1016/j.tracli.2018.08.006.

47. Chiueh CC. Iron overload, oxidative stress, and axonal dystrophy in brain disorders. Pediatr Neurol. 2001;25(2):138–47. https://doi.org/10.1016/s0887-8994(01)00266-1.

48. Levi S, Cozzi A, Santambrogio P. Iron pathophysiology in neurodegeneration with brain iron accumulation. Adv Exp Med Biol. 2019;1173:153–77. https://doi.org/10.1007/978-981-13-9589-5_9.

49. Yan N, Zhang J. Iron metabolism, ferroptosis, and the links with Alzheimer's disease. Front Neurosci. 2019;13:1443. https://doi.org/10.3389/fnins.2019.01443.

50. Gao D, Ripley S, Weichenthal S, Godri Pollitt KJ. Ambient particulate matter oxidative potential: chemical determinants, associated health effects, and strategies for risk management. Free Radical Biol Med. 2020;151:7–25. https://doi.org/10.1016/j.freeradbiomed.2020.04.028.

51. Lonnerdal B, Georgieff MK, Hernell O. Developmental physiology of iron absorption, homeostasis, and metabolism in the healthy term infant. J Pediatr. 2015;167(4 Suppl):S8-14. https://doi.org/10.1016/j.jpeds.2015.07.014.

52. Modabbernia A, Arora M, Reichenberg A. Environmental exposure to metals, neurodevelopment, and psychosis. Curr Opin Pediatr. 2016;28(2):243–9. https://doi.org/10.1097/MOP.0000000000000332.

53. Rodríguez-Barranco M, Lacasaña M, Aguilar-Garduño C, Alguacil J, Gil F, González-Alzaga B, et al. Association of arsenic, cadmium and manganese exposure with neurodevelopment and behavioural disorders in children: a systematic review and meta-analysis. Sci Total Environ. 2013;454–455:562–77. https://doi.org/10.1016/j.scitotenv.2013.03.047.

54. Fiore M, Barone R, Copat C, Grasso A, Cristaldi A, Rizzo R, et al. Metal and essential element levels in hair and association with autism severity. J Trace Elem Med Biol. 2020;57:126409. https://doi.org/10.1016/j.jtemb.2019.126409.

55. Fiłon J, Ustymowicz-Farbiszewska J, Krajewska-Kułak E. Analysis of lead, arsenic and calcium content in the hair of children with autism spectrum disorder. BMC Public Health. 2020;20(1):383. https://doi.org/10.1186/s12889-020-08496-w.

56. Palmieri L, Papaleo V, Porcelli V, Scarcia P, Gaita L, Sacco R, et al. Altered calcium homeostasis in autism-spectrum disorders: evidence from biochemical and genetic studies of the mitochondrial aspartate/glutamate carrier AGC1. Mol Psychiatry. 2010;15(1):38–52. https://doi.org/10.1038/mp.2008.63.

57. Shayganfard M. Are essential trace elements effective in modulation of mental disorders? update and perspectives. Biol Trace Elem Res. 2021. https://doi.org/10.1007/s12011-021-02733-y.

58. Palmieri L, Persico AM. Mitochondrial dysfunction in autism spectrum disorders: cause or effect? Biochim Biophys Acta. 2010;1797(6–7):1130–7. https://doi.org/10.1016/j.bbabio.2010.04.018.

59. Skalny AV, Simashkova NV, Skalnaya AA, Klyushnik TP, Zhegalova IV, Grabeklis AR, et al. Trace element levels are associated with neuroinflammatory markers in children with autistic spectrum disorder. J Trace Elem Med Biol. 2018;50:622–8. https://doi.org/10.1016/j.jtemb.2018.04.031.

60. Costa-Mallen P, Gatenby C, Friend S, Maravilla KR, Hu SC, Cain KC, et al. Brain iron concentrations in regions of interest and relation with serum iron levels in Parkinson disease. J Neurol Sci. 2017;378:38–44. https://doi.org/10.1016/j.jns.2017.04.035.

61. Degremont A, Jain R, Philippou E, Latunde-Dada GO. Brain iron concentrations in the pathophysiology of children with attention deficit/hyperactivity disorder: a systematic review. Nutr Rev. 2021;79(5):615–26. https://doi.org/10.1093/nutrit/nuaa065.

62. Gao L, Jiang Z, Cai Z, Cai M, Zhang Q, Ma Y, et al. Brain iron deposition analysis using susceptibility weighted imaging and its association with body iron level in patients with mild cognitive impairment. Mol Med Rep. 2017;16(6):8209–15. https://doi.org/10.3892/mmr.2017.7668.

63. Genoud S, Senior AM, Hare DJ, Double KL. Meta-analysis of copper and iron in Parkinson's disease brain and biofluids. Mov Disord. 2020;35(4):662–71. https://doi.org/10.1002/mds.27947.

64. Nischwitz V, Berthele A, Michalke B. Speciation analysis of selected metals and determination of their total contents in paired serum and cerebrospinal fluid samples: an approach to investigate the permeability of the human blood-cerebrospinal fluid-barrier. Anal Chim Acta. 2008;627(2):258–69. https://doi.org/10.1016/j.aca.2008.08.018.

65. Ghio AJ, Stoneheurner J, McGee JK, Kinsey JS. Sulfate content correlates with iron concentrations in ambient air pollution particles. Inhal Toxicol. 1999;11(4):293–307. https://doi.org/10.1080/089583799197104.

66. Watson AY, Brain JD. The effect of SO2 on the uptake of particles by mouse bronchial epithelium. Exp Lung Res. 1980;1(1):67–87. https://doi.org/10.3109/01902148009057514.

67. Allen JL, Liu X, Weston D, Conrad K, Oberdorster G, Cory-Slechta DA. Consequences of developmental exposure to concentrated ambient ultrafine particle air pollution combined with the adult paraquat and maneb model of the Parkinson's disease phenotype in male mice. Neurotoxicology. 2014;41:80–8. https://doi.org/10.1016/j.neuro.2014.01.004.

68. Allen JL, Liu X, Weston D, Prince L, Oberdorster G, Finkelstein JN, et al. Developmental exposure to concentrated ambient ultrafine particulate matter air pollution in mice results in persistent and sex-dependent behavioral neurotoxicity and glial activation. Toxicol Sci. 2014;140(1):160–78. https://doi.org/10.1093/toxsci/kfu059.

69. Cory-Slechta DA, Sobolewski M, Marvin E, Conrad K, Merrill A, Anderson T, et al. The impact of inhaled ambient ultrafine particulate matter on developing brain: potential importance of elemental contaminants. Toxicol Pathol. 2019;47(8):976–92. https://doi.org/10.1177/0192623319878400.

70. Sobolewski M, Varma G, Adams B, Anderson DW, Schneider JS, Cory-Slechta DA. Developmental lead exposure and prenatal stress result in sex-specific reprogramming of adult stress physiology and epigenetic profiles in brain. Toxicol Sci. 2018;163(2):478–89. https://doi.org/10.1093/toxsci/kfy046.

71. Cory-Slechta DA, Sobolewski M, Varma G, Schneider JS. Developmental lead and/or prenatal stress exposures followed by different types of behavioral experience result in the divergence of brain epigenetic profiles in a sex, brain region, and time-dependent manner: implications

Sobolewski *et al. Particle and Fibre Toxicology*   (2022) 19:56

Page 18 of 19

for neurotoxicology. Curr Opin Toxicol. 2017;6:60–70. https://doi.org/10.1016/j.cotox.2017.09.004.

72. Allen JL, Oberdorster G, Morris-Schaffer K, Wong C, Klocke C, Sobolewski M, et al. Developmental neurotoxicity of inhaled ambient ultrafine particle air pollution: parallels with neuropathological and behavioral features of autism and other neurodevelopmental disorders. Neurotoxicology. 2017;59:140–54. https://doi.org/10.1016/j.neuro.2015.12.014.

73. Klocke C, Allen JL, Sobolewski M, Mayer-Proschel M, Blum JL, Lauterstein D, et al. Neuropathological consequences of gestational exposure to concentrated ambient fine and ultrafine particles in the mouse. Soc Toxicol. 2017;156(2):492–508.

74. Morris-Schaffer K, Sobolewski M, Allen JL, Marvin E, Yee M, Arora M, et al. Effect of neonatal hyperoxia followed by concentrated ambient ultrafine particle exposure on cumulative learning in C57Bl/6J mice. Neurotoxicology. 2018;67:234–44. https://doi.org/10.1016/j.neuro.2018.06.006.

75. Morris-Schaffer K, Sobolewski M, Welle K, Conrad K, Yee M, O'Reilly MA, et al. Cognitive flexibility deficits in male mice exposed to neonatal hyperoxia followed by concentrated ambient ultrafine particles. Neurotoxicol Teratol. 2018;70:51–9.

76. Sobolewski M, Anderson T, Conrad K, Marvin E, Klocke C, Morris-Schaffer K, et al. Developmental exposures to ultrafine particle air pollution reduces early testosterone levels and adult male social novelty preference: risk for children's sex-biased neurobehavioral disorders. Neurotoxicology. 2018;68:203–11.

77. Oberdorster G, Finkelstein JN, Johnston C, Gelein R, Cox C, Baggs R, et al. Acute pulmonary effects of ultrafine particles in rats and mice. In Health effects institute research report, vol. 96. Cambridge MA: Health Effects Institute; 2000.

78. Wong JM, Malec PA, Mabrouk OS, Ro J, Dus M, Kennedy RT. Benzoyl chloride derivatization with liquid chromatography-mass spectrometry for targeted metabolomics of neurochemicals in biological samples. J Chromatogr A. 2016;1446:78–90. https://doi.org/10.1016/j.chroma.2016.04.006.

79. Morris G, Berk M, Carvalho AF, Maes M, Walker AJ, Puri BK. Why should neuroscientists worry about iron? the emerging role of ferroptosis in the pathophysiology of neuroprogressive diseases. Behav Brain Res. 2018;341:154–75. https://doi.org/10.1016/j.bbr.2017.12.036.

80. Reichert CO, de Freitas FA, Sampaio-Silva J, Rokita-Rosa L, Barros PL, Levy D, et al. Ferroptosis mechanisms involved in neurodegenerative diseases. Int J Mol Sci. 2020. https://doi.org/10.3390/ijms21228765.

81. Moos T, Rosengren Nielsen T, Skjorringe T, Morgan EH. Iron trafficking inside the brain. J Neurochem. 2007;103(5):1730–40. https://doi.org/10.1111/j.1471-4159.2007.04976.x.

82. Dallman PR, Spirito RA. Brain iron in the rat: extremely slow turnover in normal rats may explain long-lasting effects of early iron deficiency. J Nutr. 1977;107(6):1075–81. https://doi.org/10.1093/jn/107.6.1075.

83. Fang T, Guo H, Zeng L, Verma V, Nenes A, Weber RJ. highly acidic ambient particles, soluble metals, and oxidative potential: a link between sulfate and aerosol toxicity. Environ Sci Technol. 2017;51(5):2611–20. https://doi.org/10.1021/acs.est.6b06151.

84. Oakes M, Ingall ED, Lai B, Shafer MM, Hays MD, Liu ZG, et al. Iron solubility related to particle sulfur content in source emission and ambient fine particles. Environ Sci Technol. 2012;46(12):6637–44. https://doi.org/10.1021/es300701c.

85. Bartzokis G, Tishler TA, Lu PH, Villablanca P, Altshuler LL, Carter M, et al. Brain ferritin iron may influence age- and gender-related risks of neurodegeneration. Neurobiol Aging. 2007;28(3):414–23. https://doi.org/10.1016/j.neurobiolaging.2006.02.005.

86. Persson N, Wu J, Zhang Q, Liu T, Shen J, Bao R, et al. Age and sex related differences in subcortical brain iron concentrations among healthy adults. Neuroimage. 2015;122:385–98. https://doi.org/10.1016/j.neuroimage.2015.07.050.

87. Domellof M, Lonnerdal B, Dewey KG, Cohen RJ, Rivera LL, Hernell O. Sex differences in iron status during infancy. Pediatrics. 2002;110(3):545–52.

88. Lopes de Andrade V, Marreilha Dos Santos AP, Aschner M. Neurotoxicity of metal mixtures. Adv Neurotoxicol. 2021;5:329–64. https://doi.org/10.1016/bs.ant.2020.12.003.

89. Jomova K, Vondrakova D, Lawson M, Valko M. Metals, oxidative stress and neurodegenerative disorders. Mol Cell Biochem. 2010;345(1–2):91–104. https://doi.org/10.1007/s11010-010-0563-x.

90. Laakso A, Vilkman H, Bergman J, Haaparanta M, Solin O, Syvälahti E, et al. Sex differences in striatal presynaptic dopamine synthesis capacity in healthy subjects. Biol Psychiatry. 2002;52(7):759–63. https://doi.org/10.1016/s0006-3223(02)01369-0.

91. Becker JB. Gender differences in dopaminergic function in striatum and nucleus accumbens. Pharmacol Biochem Behav. 1999;64(4):803–12. https://doi.org/10.1016/s0091-3057(99)00168-9.

92. Walker QD, Rooney MB, Wightman RM, Kuhn CM. Dopamine release and uptake are greater in female than male rat striatum as measured by fast cyclic voltammetry. Neuroscience. 2000;95(4):1061–70. https://doi.org/10.1016/s0306-4522(99)00500-x.

93. Andersen SL, Rutstein M, Benzo JM, Hostetter JC, Teicher MH. Sex differences in dopamine receptor overproduction and elimination. NeuroReport. 1997;8(6):1495–8. https://doi.org/10.1097/00001756-199704140-00034.

94. Hare DJ, Double KL. Iron and dopamine: a toxic couple. Brain. 2016;139(4):1026–35. https://doi.org/10.1093/brain/aww022.

95. Dichtl S, Haschka D, Nairz M, Seifert M, Volani C, Lutz O, et al. Dopamine promotes cellular iron accumulation and oxidative stress responses in macrophages. Biochem Pharmacol. 2018;148:193–201. https://doi.org/10.1016/j.bcp.2017.12.001.

96. Badillo-Ramírez I, Saniger JM, Rivas-Arancibia S. 5-S-cysteinyl-dopamine, a neurotoxic endogenous metabolite of dopamine: Implications for Parkinson's disease. Neurochem Int. 2019;129:104514. https://doi.org/10.1016/j.neuint.2019.104514.

97. Davenport EC, Szulc BR, Drew J, Taylor J, Morgan T, Higgs NF, et al. Autism and schizophrenia-associated CYFIP1 regulates the balance of synaptic excitation and inhibition. Cell Rep. 2019;26(8):2037-51.e6. https://doi.org/10.1016/j.celrep.2019.01.092.

98. Davis AM, Ward SC, Selmanoff M, Herbison AE, McCarthy MM. Developmental sex differences in amino acid neurotransmitter levels in hypothalamic and limbic areas of rat brain. Neuroscience. 1999;90(4):1471–82. https://doi.org/10.1016/S0306-4522(98)00511-9.

99. Al-Suwailem E, Abdi S, El-Ansary A. Sex differences in the glutamate signaling pathway in juvenile rats. J Neurosci Res. 2018;96(3):459–66. https://doi.org/10.1002/jnr.24144.

100. Chang L, Jiang CS, Ernst T. Effects of age and sex on brain glutamate and other metabolites. Magn Reson Imaging. 2009;27(1):142–5. https://doi.org/10.1016/j.mri.2008.06.002.

101. Maher P. Potentiation of glutathione loss and nerve cell death by the transition metals iron and copper: implications for age-related neurodegenerative diseases. Free Radic Biol Med. 2018;115:92–104. https://doi.org/10.1016/j.freeradbiomed.2017.11.015.

102. Dixon SJ, Lemberg KM, Lamprecht MR, Skouta R, Zaitsev EM, Gleason CE, et al. Ferroptosis: an iron-dependent form of nonapoptotic cell death. Cell. 2012;149(5):1060–72. https://doi.org/10.1016/j.cell.2012.03.042.

103. Banerjee R, Vitvitsky V, Garg SK. The undertow of sulfur metabolism on glutamatergic neurotransmission. Trends Biochem Sci. 2008;33(9):413–9. https://doi.org/10.1016/j.tibs.2008.06.006.

104. Vitvitsky V, Thomas M, Ghorpade A, Gendelman HE, Banerjee R. A functional transsulfuration pathway in the brain links to glutathione homeostasis. J Biol Chem. 2006;281(47):35785–93. https://doi.org/10.1074/jbc.M602799200.

105. Burger A, Kotze MJ, Stein DJ, Janse van Rensburg S, Howells FM. The relationship between measurement of in vivo brain glutamate and markers of iron metabolism A proton magnetic resonance spectroscopy study in healthy adults. Eur J Neurosci. 2020;51(4):984–90. https://doi.org/10.1111/ejn.14583.

106. Wood JD, Kurylo E, Geddes JW. Methionine-induced changes in glutamate, aspartate, glutamine, and gamma-aminobutyrate levels in brain tissue. J Neurochem. 1985;45(3):777–83. https://doi.org/10.1111/j.1471-4159.1985.tb04060.x.

107. Machado FR, Ferreira AG, da Cunha AA, Tagliari B, Mussulini BH, Wofchuk S, et al. Homocysteine alters glutamate uptake and Na+, K+-ATPase activity and oxidative status in rats hippocampus: protection by vitamin C. Metab Brain Dis. 2011;26(1):61–7. https://doi.org/10.1007/s11011-011-9232-3.

108. Abushik PA, Niittykoski M, Giniatullina R, Shakirzyanova A, Bart G, Fayuk D, et al. The role of NMDA and mGluR5 receptors in calcium mobilization and neurotoxicity of homocysteine in trigeminal and cortical neurons and glial cells. J Neurochem. 2014;129(2):264–74. https://doi.org/10.1111/jnc.12615.

109. Tisato V, Silva JA, Longo G, Gallo I, Singh AV, Milani D, et al. Genetics and epigenetics of one-carbon metabolism pathway in autism spectrum disorder: a sex-specific brain epigenome? Genes (Basel). 2021. https://doi.org/10.3390/genes12050782.

110. Campesi I, Carru C, Zinellu A, Occhioni S, Sanna M, Palermo M, et al. Regular cigarette smoking influences the transsulfuration pathway, endothelial function, and inflammation biomarkers in a sex-gender specific manner in healthy young humans. Am J Transl Res. 2013;5(5):497–509.

111. Fukagawa NK, Martin JM, Wurthmann A, Prue AH, Ebenstein D, O'Rourke B. Sex-related differences in methionine metabolism and plasma homocysteine concentrations. Am J Clin Nutr. 2000;72(1):22–9. https://doi.org/10.1093/ajcn/72.1.22.

112. Vitvitsky V, Prudova A, Stabler S, Dayal S, Lentz SR, Banerjee R. Testosterone regulation of renal cystathionine beta-synthase: implications for sex-dependent differences in plasma homocysteine levels. Am J Physiol Renal Physiol. 2007;293(2):F594-600. https://doi.org/10.1152/ajprenal.00171.2007.

113. Klocke C, Allen JL, Sobolewski M, Blum JL, Zelikoff JT, Cory-Slechta DA. Exposure to fine and ultrafine particulate matter during gestation alters postnatal oligodendrocyte maturation, proliferation capacity, and myelination. Neurotoxicology. 2017. https://doi.org/10.1016/j.neuro.2017.10.004.

Publisher's Note